Structural Models for the Geology of the Hanna Basin, Carbon County, Wyoming

Karen M. Aydinian

Senior Integrative Exercise

April 1, 2008

Submitted in partial fulfillment of the requirements for a Bachelor of Arts degree from Carleton College, Northfield, Minnesota

Table of Contents

Abstract

Introduction

Geologic Setting

Methods

Discussion

- Trishear and the Hanna Basin
- “Evolved” Triangle Zones and the Hanna Basin
- The Cross Sections

Conclusion

Acknowledgements

References

Appendix: Stratigraphic Units of the Study Area

Abstract

The Hanna Basin in Carbon County, Wyoming, poses unusual and little studied structural problems. Several hypotheses have been proposed previously to explain the geology in the basin, but no adequate strike and dip data had been collected to support the construction of cross-sections. This paper explores the previously proposed models, which include several north-verging out-of-the-basin thrust faults, and introduces several new possibilities with faults verging both north and south. Constructed cross-sections demonstrate the varying viability of these models as explanations for the geologic structures mapped at the surface of the northern boundary of the Hanna Basin. Both trishear and evolved triangle zones are discussed as means to model deformation styles in this basin. The most viable model based upon the cross-sections constructed for this paper involves a series of north-verging, out-of-the-basin thrust faults which place younger Tertiary/Cretaceous strata on older Cretaceous strata and create a triangle zone between the smaller north-verging thrusts, the south-verging Shirley Thrust, and a deep, south-verging blind master thrust.

Keywords
Hanna Basin, Laramide basin, trishear, triangle zone, Shirley Thrust, Horseshoe Ridge Anticline

Introduction

The Hanna Basin in Carbon County, Wyoming, is a structurally complex but inadequately studied area. The Hanna Basin is a small basin, formed during the Laramide orogeny, in the Rocky Mountain foreland of south-central Wyoming (Lillegraven, 1996). It is anomalous for a basin formed in the Laramide because it is very small in comparison to other Laramide-age basins, and it has very thick, synorogenic strata (Lillegraven, 2004). The goal of this project is to examine the structural mechanisms that caused the present geologic setting of the northern Hanna Basin, just south of the Shirley Mountains, and to reconstruct the geologic history of the area. A greater understanding of the structural geology of the Hanna Basin can lead to the opportunity to discover more about the relationships between Laramide activity in the Colorado Plateau to the south and activity in north-central and northwestern Wyoming, such as in the Wind River and Owl Creek ranges.

There are several previously proposed hypotheses to test in this region. One is that the northern Hanna Basin is a simple, fault-bounded block of Cretaceous sediments that has been rotated to vertical by a deep fault mechanism (Heller). If this is so, there should be no intermediate dip values between 30º and 65º, those recorded in a previous study (Lillegraven, 1996), in sections 24, 19, 30, and 29 on the USGS Schneider Ridge Quadrangle (**Figure 1**). Another proposed model is that the vertical beds are part of a triangle structure between a splay fault off a deep, south-verging blind thrust and a shallow, north-verging "out-of-the-basin" fault (Lillegraven, 2004).

Geologic Setting

The Hanna Basin is bounded on the north by the Shirley Thrust, a high-angle, basement involved reverse fault (Lillegraven, 1996). This fault brought up the Shirley Mountains, which have been eroded to expose the Precambrian basement (Lillegraven, 1996). The Shirley Thrust terminates to the east in a fold of Upper Cretaceous units (Lillegraven, 1996). Directly east of the Shirley Mountains, northeast of the study area, are the Freezeout Hills, composed of folded and exposed Paleozoic and Mesozoic strata (Lillegraven, 1996). East from the Hanna Basin is a series of *en echelon*, basement-involved asymmetric anticlines, such as the Flat Top and Como Bluff anticlines (Lillegraven, 1996). Northwest of the Hanna Basin are the Seminoe Mountains and the Ferris Mountains. The E-W trending elongation of the Ferris, Seminoe, Shirley, and Freezeout uplifts are part of the southeastern flank of the Sweetwater arch (Lillegraven, 1996).

The majority of the study area is composed of the exposed Tertiary/Cretaceous Ferris/Hanna Formations. The Ferris and Hanna formations in the study area are primarily coarse-grained to very coarse-grained sandstones, which become more conglomeritic in nature to the south. The exposed outcrops are large channel flows, probably indicative of a braided stream environment. These outcrops feature flat tops, broad scour surfaces on the bottom, and crossbedding. In the area just south of Schneider Ridge, the beds dip between 65º to the south and 90º. There is a shift in orientation of the Ferris and Hanna formations about 2 miles south of the base of Schneider Ridge, on the south side of a broad valley through which County Road 219 (Hanna-Leo Road) runs. The rocks in the southern part of the basin dip between 20º and 35º to the southeast. There are several locations in the study area in which these two orientations are juxtaposed. This was previously mapped as a possible out-of-the-basin fault, which places younger strata on older strata, by Lillegraven (1996).

Methods

Strike and dip data was collected for this area along three major north-south transects (**Figure 2**). Several locations, such as the top of Schneider Ridge, the channel “fins” of the Ferris/Hanna Formations, and the badlands to the south of the Hanna-Leo Road were mapped in greater detail. Figure 2 shows a representative portion of orientations of bedding in the study area. The stratigraphy along these transects was mapped by Lillegraven (1996) and can be seen, along with Lillegraven’s structural interpretations based on stratigraphic section, in Figure 3.

Figure 2 displays structures that were hypothesized in the field based on strike and dip data alone. Figures 4, 5, and 6 are the different interpretations presented in the cross-section models of this paper. Based on these three scenarios of fault vergences along the transects, the cross-sections represent at least five models of varying viability and plausibility to explain the geologic structures in the study area.

The cross-sections were constructed using the principle of constant thickness of rock layers. The lines in each cross-section represent bedding planes rather than formation boundaries. Each of these lines was drawn using the measured dip angle for that point along the transect. To make these cross-sections viable, the bedded layers must have a constant thickness throughout the cross-section. This method assumes that a constant thickness for a rock unit ensures a constant volume for that particular unit. In order to consider these cross-sections balanced, the length of bedding layers both in the deformed state and restored cross-sections would need to match. This paper considers deformed state models only.

The cross-sections presented in this paper are not balanced. Four out of the five models have major volume problems that would need to be resolved in future studies. These volume problems suggest that some of these models do not fit the collected data well enough to be considered as a final interpretation, but may work if particular details are changed slightly. The cross-sections serve as a preliminary examination of different structural possibilities; rather than prove one model, they seek to eliminate those that do not work well.

Discussion

Trishear and the Hanna Basin

The cross-sections featured in this paper assume little to no deformation of rock units themselves. As a whole, these units bend by slipping along bedding planes in incompetent shales between the sturdier sandstone layers. Other than this sliding and bending, the rock layers undergo little individual deformation.

The trishear model expounded by Erslev (1991) explains the deformation as seen in nature more accurately than the simplified model used for this paper. In the trishear model, the dips of beds are not uniform throughout the unit, as they are in the cross-sections of this paper. Instead, the dips rotate so that beds in closer proximity to the fault have dips that are close to that of the fault plane itself (**Figure 7**). In order to accommodate this, beds close to the fault elongate and shear, while minor folds and thrusts develop to accommodate shortening. Trishear allows for the possibility of heterogeneous deformation, while the cross-sections in this paper are homogeneous.

The trishear model is one possible deformation style to explain the complexities of the Hanna Basin. When applied to the study area, the Shirley Thrust breaks to the surface off the deep blind thrust. The Shirley Thrust causes the sediments above it to form a fault propagation fold. The Cretaceous sediments, such as the members of the Mesaverde group, would fold and shear as a result of compression from movement along the blind master fault. As this structure is unroofed, the Paleozoic and Mesozoic sediments overlaying the Precambrian erode, exposing the metamorphic core in the north of the study area.

The overturned beds of Schneider Ridge might be the result of a smaller fault that originated in the forelimb of the major fold. Shear in the center of the fold near the fault plane caused these units to lengthen and overturn, and may have been further overturned as the south-verging fault moved over them.

A possibility that fits with the trishear model is that there is an erosional unconformity exposing the forelimb of the fault propagation fold (Hauge). As the fold was lifted and exposed, the eroded sediment filled the basin. The system remained active, rotating the earlier basin fill as the fold continued to propagate and dumping newer basin fill along an angular unconformity in the tilted basin. When the system stopped, the sediment continued to erode, eventually exposing the forelimb of the fold. Figure 9 shows how the erosional uncomformity can account for the exposure of beds with varying dips across the basin.

"Evolved" Triangle Zones and the Hanna Basin

The evolved triangle zone model proposed by Sterne (2006) provides a balanced and restorable model to explain anomalous younger-over-older relationships like those seen in the Hanna Basin. Sterne's triangle zone model differs from Erslev's in the formation of fault propogation folds. While Erslev's trishear model involves shear of the layers closest to the fault driving the fold, the triangle zone model features homogeneous propogation folds and prominent backthrusts which are caused by crowding in front of the major thrust fault. These backthrusts are foreland dipping, hinterland verging, tend to run parallel to bedding in the hanging wall and cut across bedding in the footwall, and cause younger-on-older relationships (Sterne, 2006). This scenario would correspond to the orientation of the Hanna-Leo Road fault drawn in models 1-4 of the cross-sections examined in this paper. Several out-of-the-basin backthrusts formed as a result of crowding in the basin. These faults would place younger Tertiary rocks on older Cretaceous sediment. According to the triangle zone model (Sterne, 2006) these faults would occur in several parts of the basin, and a passive roof thrust may form over the south-verging wedge (**Figure 8**). Figure 10 illustrates the evolution of the triangle zone from an underformed state.

The faults continue to build upon each other over time and may move simultaneously, resulting in overturned bedding and faults (Sterne, 2006). The extensive overturned bedding at the base and southern side of Schneider Ridge may be a result of movement along a north-verging backthrust. The beds at the base of Schneider Ridge are only slightly overturned, but become progressively more overturned nearing the top of the ridge. The beds near the top of the ridge might have been rotated to nearly horizontal while the underlying backthrust became nearly vertical as it broke to the surface.

The Cross-Sections

Cross-section model 1 depicts a series of north-verging, out-of-the-basin thrust faults that place younger rocks on older rocks throughout the northern part of the Hanna Basin and Horseshoe and Schneider Ridges. Out of the various cross-sections attempted, this has the fewest volume problems, and accordingly would be the most promising model. This model was based on the hypothesis of Taft (1997), using the seismic data from Homan (1988). Figure 11 shows Taft's interpretation of the data.

Model 1 is an example of the triangle zone model proposed by Lillegraven et al (2004) and Sterne (2006). The Shirley Fault in the north is a high angle, south-verging splay fault off a larger, low angle blind master thrust. Figure 12 illustrates the formation of the anticline to the north of the Hanna Basin, the core of which is the Precambrian metamorphic that is now exposed as the Shirley

Mountains. The blind thrust continued to move southward, causing crowding in the basin. A series of smaller, north-verging faults formed in the basin to accommodate the crowding. One of these north-directed faults formed the anticline of Horseshoe and Schneider Ridges. Figure 13 illustrates this process in a very simplified way.

This model would label the variation in dips along the Hanna-Leo Road as a low angle, out-of-the-basin thrust fault, which is confined to the TK Ferris/Hanna Formations and places younger TK Ferris/Hanna on the steeply dipping, TK Ferris/Hanna “fins.” One possible explanation for the steep dip of the “fins” is that they are the forelimb of a north-directed fault propagation fold. This would have to have been a very large fold, and seems unlikely. A more plausible explanation is the first north-directed thrust occurred when the TK Ferris/Hanna was nearly horizontal. The next north-directed fault propagated through the footwall, tilting the previous fault slightly, as well as the layers of the TK Ferris/Hanna between the faults. In order to have achieved the steep dips between the two faults but shallow dips to the south of the Hanna-Leo Road, the second, more northerly fault might have run horizontally, parallel to bedding, several miles to the north of the first fault’s exposure at the surface, before breaking to the surface itself.

Figures 14 and 15 illustrate this model in cross-section. Both feature a syncline under the Hanna-Leo Road fault, with the “fins” rising close to vertical as the back limb of a fault propagation fold that terminates in the Horseshoe and Schneider Ridges.

Model 2 features a north-directed, out-of-the-basin thrust in the south and a south-directed splay thrust forming the Horseshoe and Schneider Ridges. This model has some significant problems; however it was the first attempt using this fault configuration. Figure 16 is a simplified timeline of events for models 2, 3, and 4, which feature the north-verging out-of-the-basin fault in the south and the south-verging splay fault at Horseshoe and Schneider Ridges.

Like model 1, model 2 has the out-of-the-basin thrust juxtaposed against much more steeply dipping layers. Whereas in model 1 these layers are the back limb of a north-directed fault propagation fold, in model 2 these layers are the limb of a basinal syncline. One of the major volume problems of this model is in these layers, just south of A' (**Figure 17**). The thickest unit undergoes significant change in thickness near the erosional surface, due in part to the anticline of Horseshoe Ridge. This anticline is formed by the south-directed splay fault off the Shirley Thrust. Underneath this splay fault is a north-leaning anticline. The tilt of this anticline does not correspond with the movement of the blind master fault, and is corrected in Figures 20 and 21. In Figure 18, the structure of Schneider Ridge is represented as a less developed section of the anticline of Horseshoe Ridge. Both Figures 18 and 19 illustrate the problem relating the anticline to the steeply dipping beds in the basin.

Model 3, like model 2, features a north-directed, out-of-the-basin fault in the south and a south-directed, deep splay fault forming the anticlines of Horseshoe and Schneider Ridges (**Figure 20**). The main difference in this model is the southernly tilt of the anticline underneath the splay fault. The half of the syncline visible between A and A' of Figure 19 is nearly upright, and so is the adjoining anticline. The anticline is truncated abruptly by the splay fault, which originates very deeply along the Shirley Thrust. The lack of a hanging wall cutoff is especially problematic.

Model 4 (**Figure 21**) corrects this problem. It is nearly the same as model 3, but the splay fault is shallower, and propagates parallel to the top of the anticline. The hanging wall cutoff below A''' would have been lifted along the Shirley Thrust and eroded away. The blind master fault developed first, forming the anticline/syncline pair seen in Figure 21. Crowding in the basin, caused by the south-directed master fault, resulted in the formation of the north-verging out-of-the-basin thrust. At some point, either before or after the start of the north-verging fault, the south-verging splay fault began, resulting in the formation of the Horseshoe Ridge anticline.

The out-of-the-basin fault originates at the blind master fault. The point at which this fault breaks upward corresponds to the “tip” of Sterne’s evolved triangle model (2006). The area between the out-of-the-basin fault and the Shirley Fault is the triangle zone.

Model 5 is only drawn on one transect, transect B (**Figure 22**). This model was my initial field hypothesis, and it is included in this paper in order to eliminate this hypothesis. Model 5 features two main south-verging faults. It is the only model to postulate that the fault along the Hanna-Leo Road is south-verging. This fault, as it is drawn, truncates the nearly vertical beds in the basin, rather than propagating parallel to bedding. This is an unlikely scenario. It is also not likely that this could be modeled as a rotated, fault-bounded block. The beds are nearly vertical, but dipping to the south and not overturned. If this block had been rotated due to movement on a south-verging blind master, the dips would be overturned to the north.

The shallower dips on the south side of the Hanna-Leo Road fault are represented in model 5 as drag from the south-verging fault. While this may be plausible with the dips, the strikes of the beds to the south of this fault are different than those to the north of the fault. This would not be merely the result of drag. Either the beds to the north or the south of the road have been rotated as a block, or there is a differently-trending fault plane or unconformity present.

Conclusion

The small size and symmetrical shape of the Hanna Basin set it apart from other Laramide basins of the eastern Rocky Mountains. Located at the convergence of the Colorado Front Range to the south and the Wind River Basin to the north, the structures of the Hanna Basin and surrounding area can be an important aspect of piecing together a cohesive sequence of events of the Laramide orogeny throughout the Rocky Mountain foreland. In order to do this, the hypotheses regarding principle stress systems and deformation styles must be correlated.

The fieldwork of this study was used to examine the previous hypotheses as to the structures of the northern boundary of the Hanna Basin, as well as to test a new hypothesis. The new hypothesis of this study proposed that the fault seen at the Hanna-Leo Road is south-verging; this model does not work well when put into cross-section. The models featuring a south-verging splay thrust at Horseshoe and Schneider Ridges and a north-verging out-of-the-basin thrust at the Hanna-Leo Road have a few problems, but cannot be eliminated. With minor changes, this fault configuration can be viable. The previously proposed hypothesis of a series of north-verging out-of-the-basin faults at Horseshoe Ridge (Taft, 1997), combined with the "evolved" triangle zone model featuring a shallow roof thrust over the out-of-the-basin thrusts (Sterne, 2006) seems to be the best fit with the data collected in this study.

Acknowledgements

I would like to thank Dr. Sarah Titus of Carleton College for her assistance with this project, as well as Dr. Art Snoke, Dr. Barbara Carrapa, Dr. Paul Heller, and Liz Hajek of the University of Wyoming for their assistance and contributions. I would like to thank Dr. Tom Hauge for offering critique of the cross-sections and suggestions for the erosional unconformity model. I would like to thank Gene Aydinian for being my field assistant with this project.

References

Erslev, E. A., 1991, TRISHEAR FAULT-PROPAGATION FOLDING: Geology, v. 19, no. 6, p. 617-620.

Gill, J. R., Merewether, E. A., and Cobban, W. A., 1970, Stratigraphy and Nomenclature of Some Upper Cretaceous and Lower Tertiary Rocks in South-Central Wyoming: Geological Survey Professional Paper 667, United States Government Printing Office.

Hauge, T., Geophysical Advisor, ExxonMobil (Retired).

Heller, P., Professor, University of Wyoming.

Homan, K. S., 1988, Structural analysis of the south flank of the Sweetwater uplift,

Carbon County, Wyoming: Baylor University, 160 p.

Lillegraven, J. A., and Snoke, A. W., 1996, A new look at the Laramide orogeny in the Seminoe and Shirley mountains, Freezeout Hills, and Hanna Basin,

south-central Wyoming, *in* Jones, R. W., ed., Public Information Circular No. 36: Cheyenne, WY, Pioneer Printing and Stationary.
Lillegraven, J. A., Snoke, Arthur W., and McKenna, Malcolm C., 2004, Tectonic and paleogeographic implications of late Laramide geologic history in the northeastern corner of Wyoming's Hanna Basin: Rocky Mountain Geology, v. 39, no. 1, p. 7-64.
Sterne, E. J., 2006, Stacked, "Evolved" Triangle Zones Along the Southeastern Flank of the the Colorado Front Range: The Mountain Geologist, v. 43, no. 1, p. 65-92.
Taft, K., 1997, Masters Thesis of Kendale Taft: University of Wyoming.

Appendix: Stratigraphic Units of the Study Area

South of the Shirley Mountains, in the northernmost part of the study area, is a succession of Cretaceous units which proceed stratigraphically younger to the south. These included both marine and nonmarine sandstones, shales, siltstones, and carbonates. Beginning with the Thermopolis Shale, Muddy Shale, Mowry Shale, Frontier Formation, and Niobrara Formation (Lillegraven, 1996). Above the Niobrara Formation is the Steele Shale, approximately 2,300 to 3,800 feet of marine limestone and bentonite, siltstones, and sandstones (Gill, 1970). Next is the Mesaverde group—Haystack Mountains Fm., Allen Ridge Formation., Pine Ridge Sandstone, and Almond Formation (Lillegraven, 1996). All but the Allen Ridge Formation are marine sandstones and shales. The Allen Ridge Formation is nonmarine sandstones, shales, and carbonates (Gill, 1970). Above the Mesaverde group is the Lewis Shale, approximately 2,200 to 2,600 feet of dark gray marine shale with interbedded sandy units (Gill, 1970). Above this is the Medicine Bow Formation, 3,000 to 6.500 feet of mostly nonmarine lenticular sandstones, siltstones, and shales. Lillegraven (1996) maps several thrust faults among these units, as there is a significant amount of strategraphic section missing in this particular part of the basin. The Medicine Bow Formation is conformabely overlain by the Cretaceous Ferris Formation.

The Hanna Basin itself is mapped as undivided Cretaceous Ferris Formation and Tertiary Hanna Formation (Figure 2). The Ferris Formation can be up to 6,500 feet thick, and can be divided into two parts (Gill, 1970). The lower 1,100 feet is congomeritic sandstone, sanstones, and shales deposited in the late Cretaceous, while the upper 5, 400 feet are Paleocene gray, brown, and yellow sandstones and coal beds (Gill, 1970). The clasts in the conglomerate are pebbles of chert, quartzite, rhyolite, and quartz latite porphyry, none of which suggest a local original source (Gill, 1970). The upper layer does not have conglomerates, and plant fossils from this layer suggest it was deposited in the early Paleocene (Gill, 1970).

The Hanna Formation unconformably overlays the Ferris Formation. This formation was deposited in the late early Paleocene, during the tectonism that formed the uplifts to the north (Lillegraven, 1996). It can be up to 13,500 feet thick in parts of the basin, and is composed of conglomerates, sandstones, shales, and coal beds (Gill, 1970). Most of the conglomerates are in the lower half of the formation, and include pebbles of chert, granite, quartzite, sandstone, Mowry Shale, and Cloverly Formation conglomerate (Gill, 1970). These are all locally derived clasts (Gill, 1970), suggesting that the formations to the north had already been uplifted and begun eroding. The Hanna Formation is most near a conformable contact with the Ferris in the center of the basin, and forms an unconformity with progressively older rocks, up to the Precambrian basement, moving out from the basin (Gill, 1970).

The Ferris and Hanna formations in the study area are primarily coarse-grained to very coarse-grained sandstones, which become more conglomeritic in nature to the south. The exposed outcrops are large channel flows, probably indicative of a braided stream environment. These outcrops feature flat tops, broad scour surfaces on the bottom, and crossbedding.

Figure 1 From Lillegraven (1996). This map shows the Hanna Basin in relation to the surrounding structures of Carbon County, Wyoming.

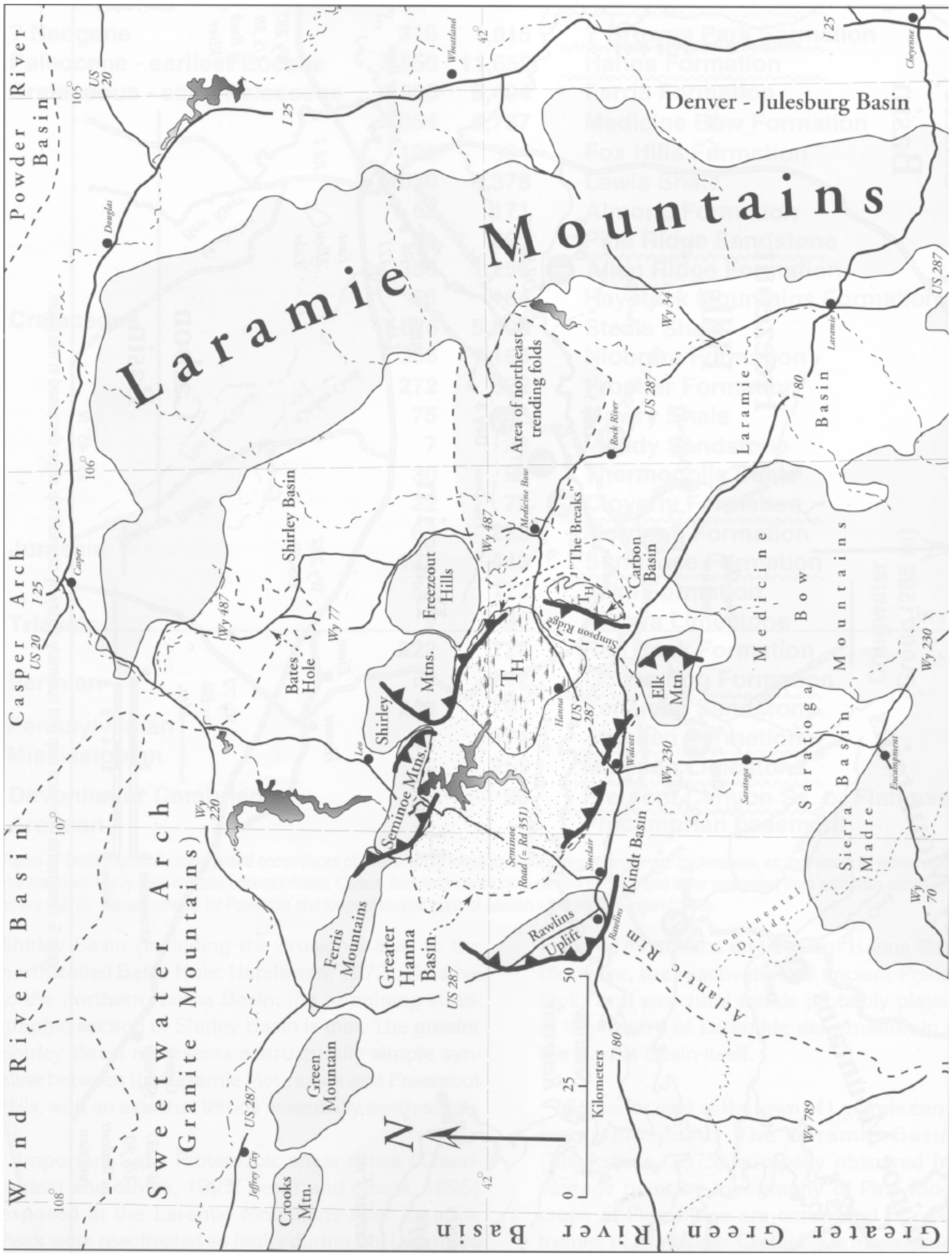
Powder River Basin
Denver - Julesburg Basin
Laramie Mountains
Casper Arch
Wind River Basin
Sweetwater Arch (Granite Mountains)
Shirley Basin
Bates Hole
Freezeout Hills
Shirley Mtns.
Area of northeast trending folds
The Breaks
Carbon Basin
Simpson Ridge
Elk Mtn.
Laramie Basin
Medicine Bow Mountains
Saratoga Basin
Sierra Madre
Seminoe Mtns.
Seminoe Road (= Rd 351)
Kindt Basin
Rawlins Uplift
Atlantic Rim
Continental Divide
Ferris Mountains
Greater Hanna Basin
Green Mountain
Crooks Mtn.
Greater Green River Basin
Casper
Douglas
Wheatland
Cheyenne
Laramie
Rock River
Medicine Bow
Hanna
Walcott
Saratoga
Encampment
Sinclair
Rawlins
Jeffrey City
Kilometers
0
25
50
N

Figure 2 a A map of the total study area. This map shows the location of the three transects: A-A''', B-B', and C-C'. The Horseshoe Ridge Anticline is indicated in the upper left corner, and the thick red lines show the location, but not orientation, of proposed faults. A representative amount of strike and dip data is included on this map.

b Smaller detail of the northwest corner of Figure 2a.

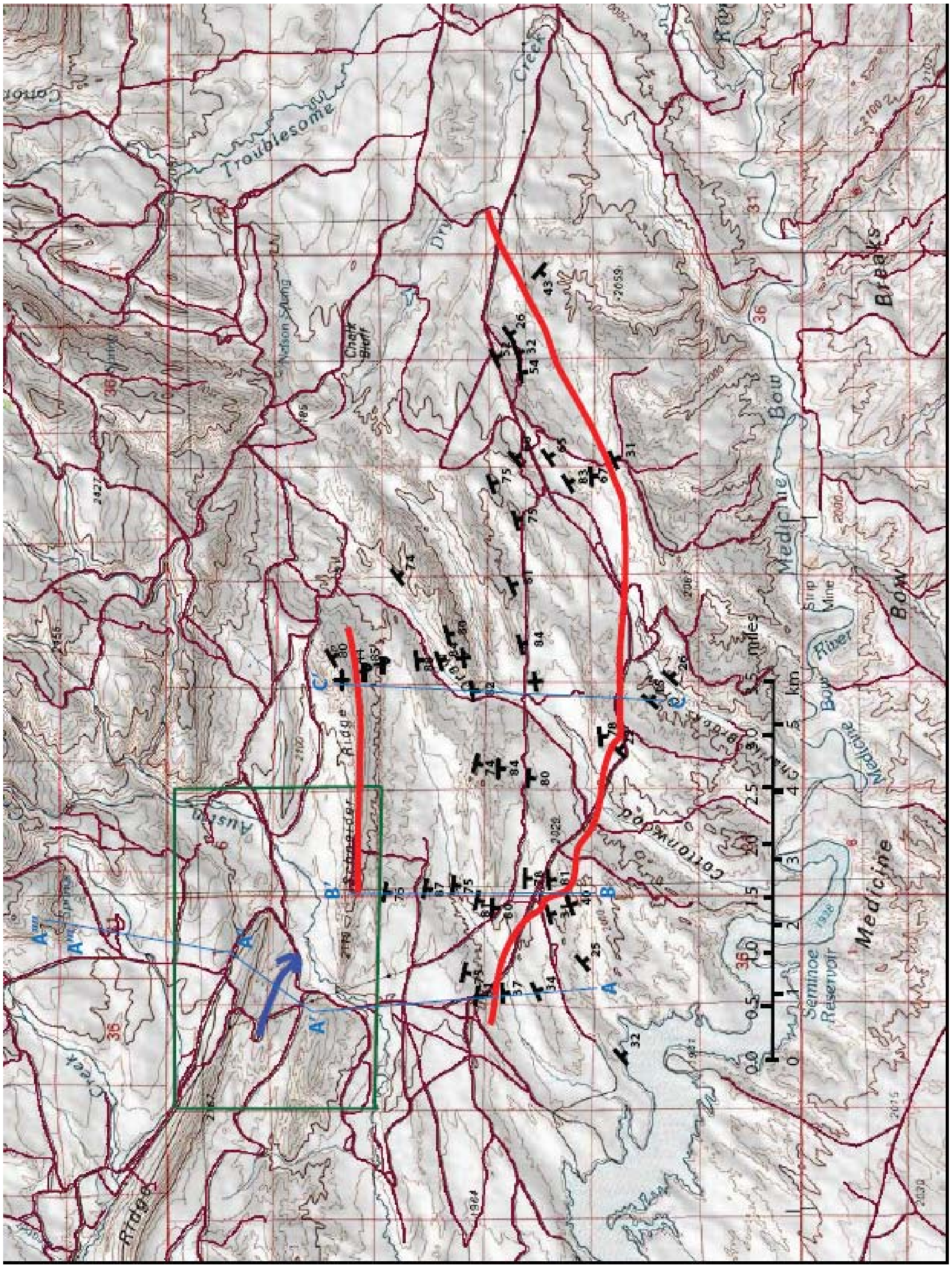
Troublesome
Creek
Dry
Nelson's Lane
Chalk Bluff
Ridge
Schneider Ridge
Austin
Cottonwood
Medicine Bow
Bow River
Medicine
Strip Mine
Breaks
Seminoe Reservoir
A
A'
A''
A'''
B
B'
C
C'
km
miles

Figure 2b

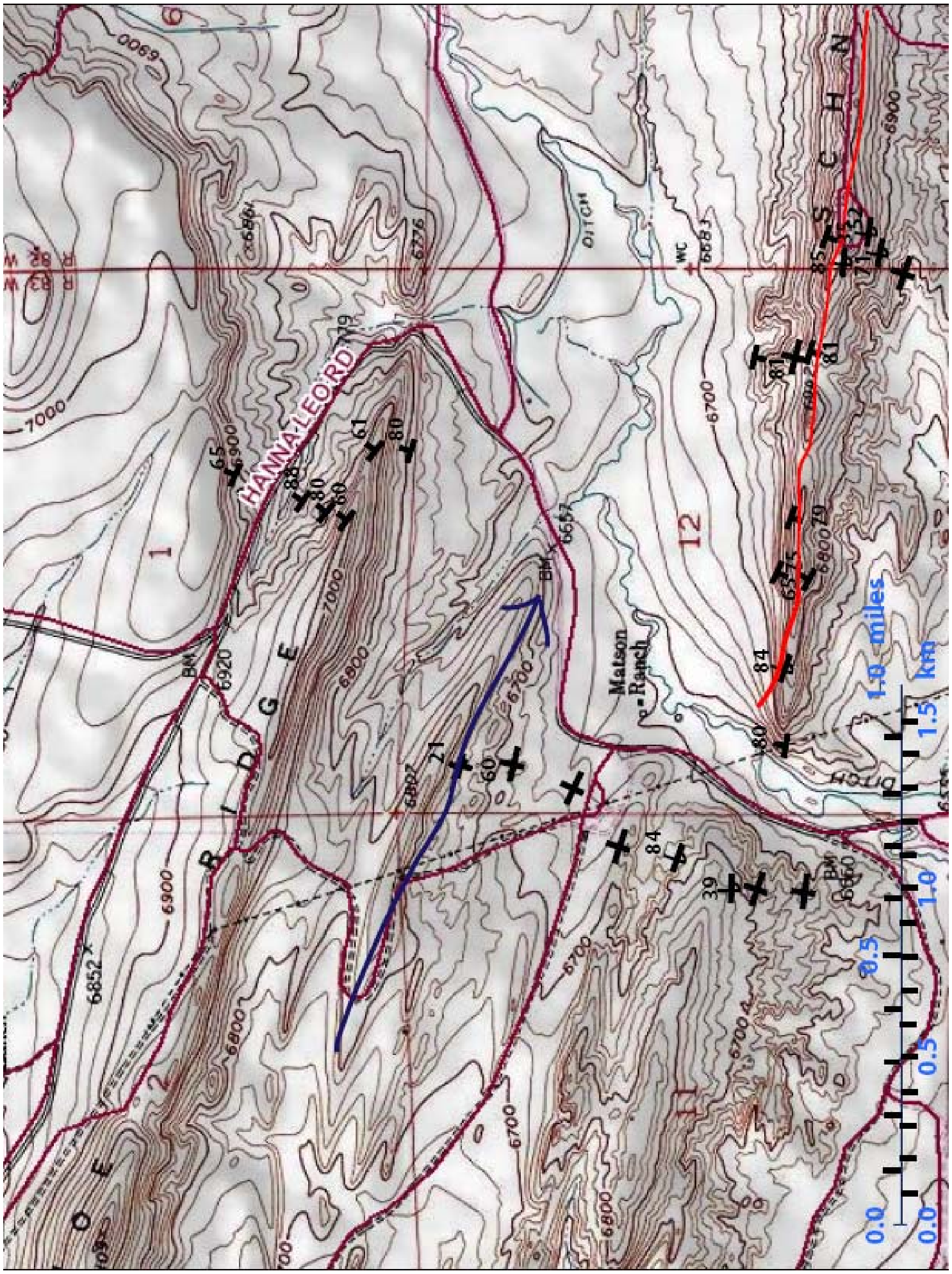
HANNA-LEO RD
R I D G E
Matson Ranch
DITCH
12
1.0 miles
km
0.0
0.5
1.0
1.5

Figure 3 From Lillegraven (1996). This map shows the mapped strategraphic section, a limited amount of strike and dip data, and the proposed structures for the study area and surrounding localities. The Hanna-Leo Road fault in the southern section on the left side is dashed, indicating uncertainty in its location or continuity. The Horseshoe Ridge Anticline is present in the middle section on the far left. The numerous faults mapped in the Horseshoe Ridge and Schneider Ridge areas are proposed based on significant amounts of missing stratigraphic section.

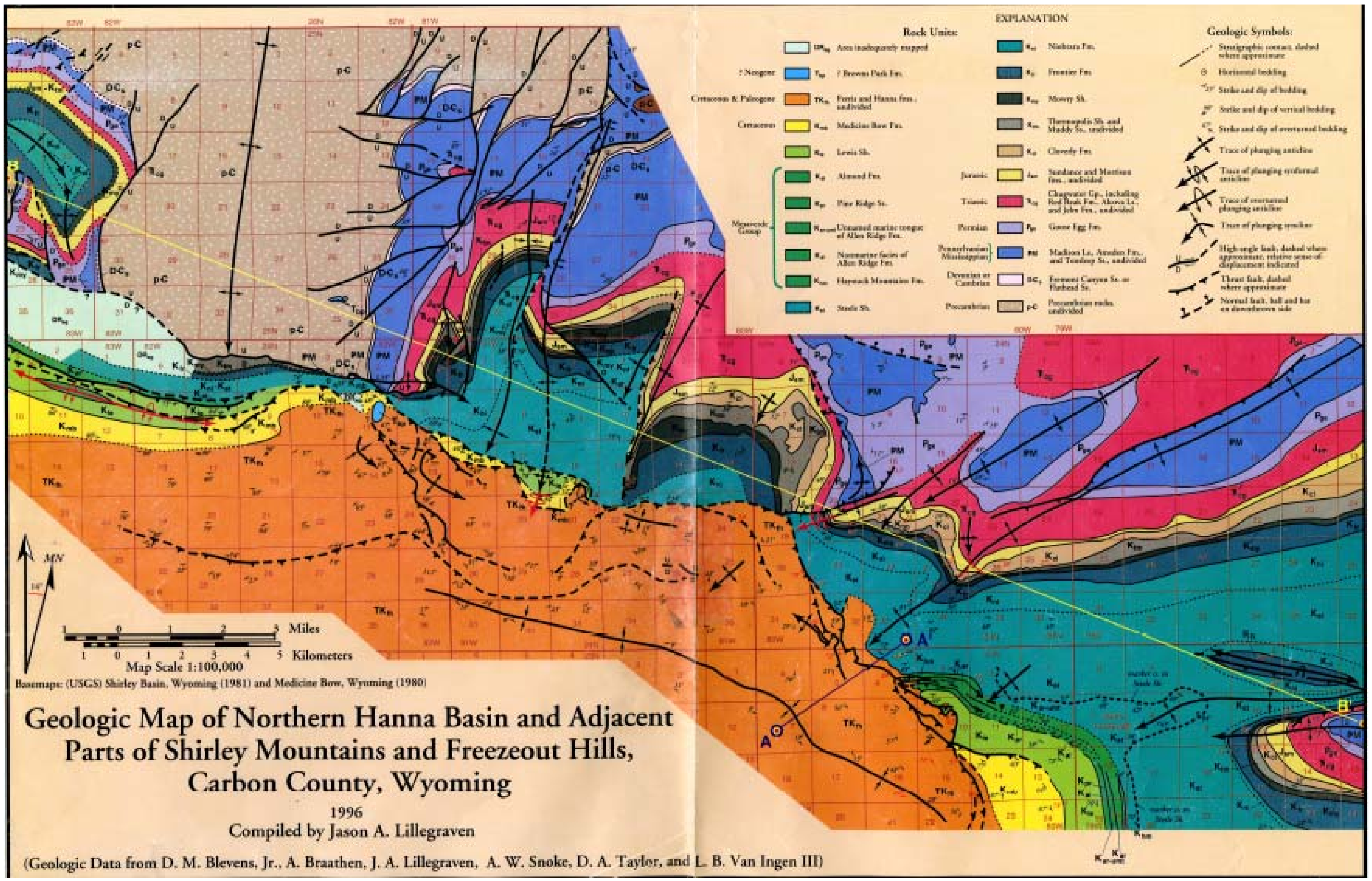

EXPLANATION
Rock Units:
Area inadequately mapped
? Neogene
? Browns Park Fm.
Cretaceous & Paleogene
Ferris and Hanna fms., undivided
Cretaceous
Medicine Bow Fm.
Lewis Sh.
Almond Fm.
Pine Ridge Ss.
Unnamed marine tongue of Allen Ridge Fm.
Nonmarine facies of Allen Ridge Fm.
Haystack Mountains Fm.
Mesaverde Group
Steele Sh.
Niobrara Fm.
Frontier Fm.
Mowry Sh.
Thermopolis Sh. and Muddy Ss., undivided
Cloverly Fm.
Jurassic
Sundance and Morrison fms., undivided
Triassic
Chugwater Gp., including Red Peak Fm., Alcova Ls., and Jelm Fm., undivided
Permian
Goose Egg Fm.
Pennsylvanian Mississippian
Madison Ls., Amsden Fm., and Tensleep Ss., undivided
Devonian or Cambrian
Fremont Canyon Ss. or Flathead Ss.
Precambrian
Precambrian rocks, undivided
Geologic Symbols:
Stratigraphic contact, dashed where approximate
Horizontal bedding
Strike and dip of bedding
Strike and dip of vertical bedding
Strike and dip of overturned bedding
Trace of plunging anticline
Trace of plunging synformal anticline
Trace of overturned plunging anticline
Trace of plunging syncline
High-angle fault, dashed where approximate, relative sense of displacement indicated
Thrust fault, dashed where approximate
Normal fault, ball and bar on downthrown side
MN
14°
Miles
Kilometers
Map Scale 1:100,000
Basemaps: (USGS) Shirley Basin, Wyoming (1981) and Medicine Bow, Wyoming (1980)
Geologic Map of Northern Hanna Basin and Adjacent Parts of Shirley Mountains and Freezeout Hills, Carbon County, Wyoming
1996
Compiled by Jason A. Lillegraven
(Geologic Data from D. M. Blevens, Jr., A. Braathen, J. A. Lillegraven, A. W. Snoke, D. A. Taylor, and L. B. Van Ingen III)

Figure 4 One possible representation of fault vergences in the study area. The Hanna-Leo Road fault in the south section of the map and the Schneider Ridge/Horseshoe Anticline fault in the north section of the map are both north-verging, out-of-the-basin faults. This structural map corresponds to the cross-sections for Model 1 in Figures 13, 14, and 15.

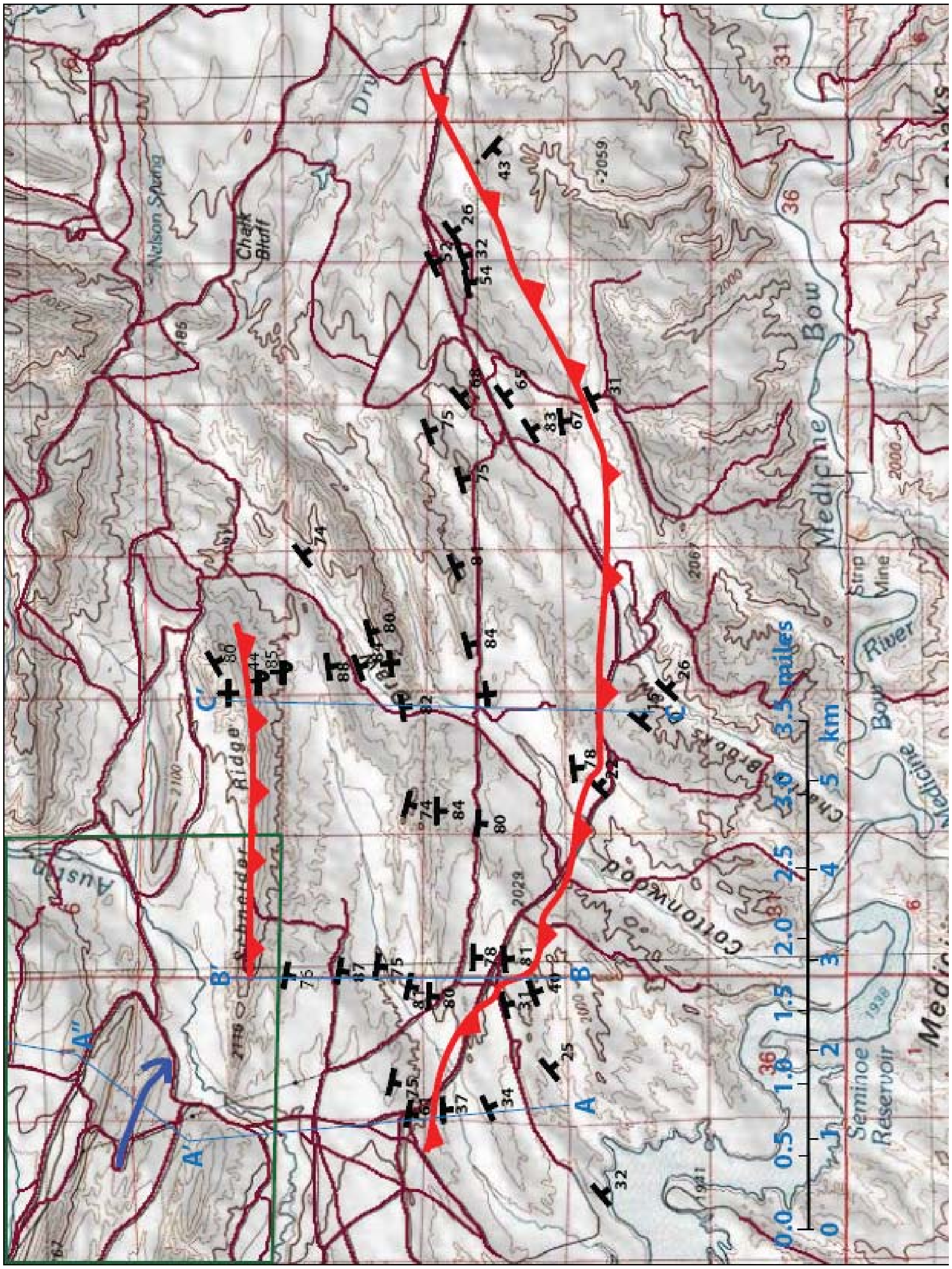

Schneider Ridge
Nelson Spring
Chalk Bluff
Cottonwood
Medicine Bow River
Seminoe Reservoir
Strip Mine
A
A'
A''
B
B'
C
C'
miles
km

Figure 5 A second representation of possible fault vergences in the study area. The Hanna-Leo Road fault is a north-verging, out-of-the-basin fault. The Schneider Ridge/Horseshoe Anticline fault is a south-directed splay thrust. This structural map corresponds to the cross-sections of Models 2, 3. and 4 in Figures 16-20.

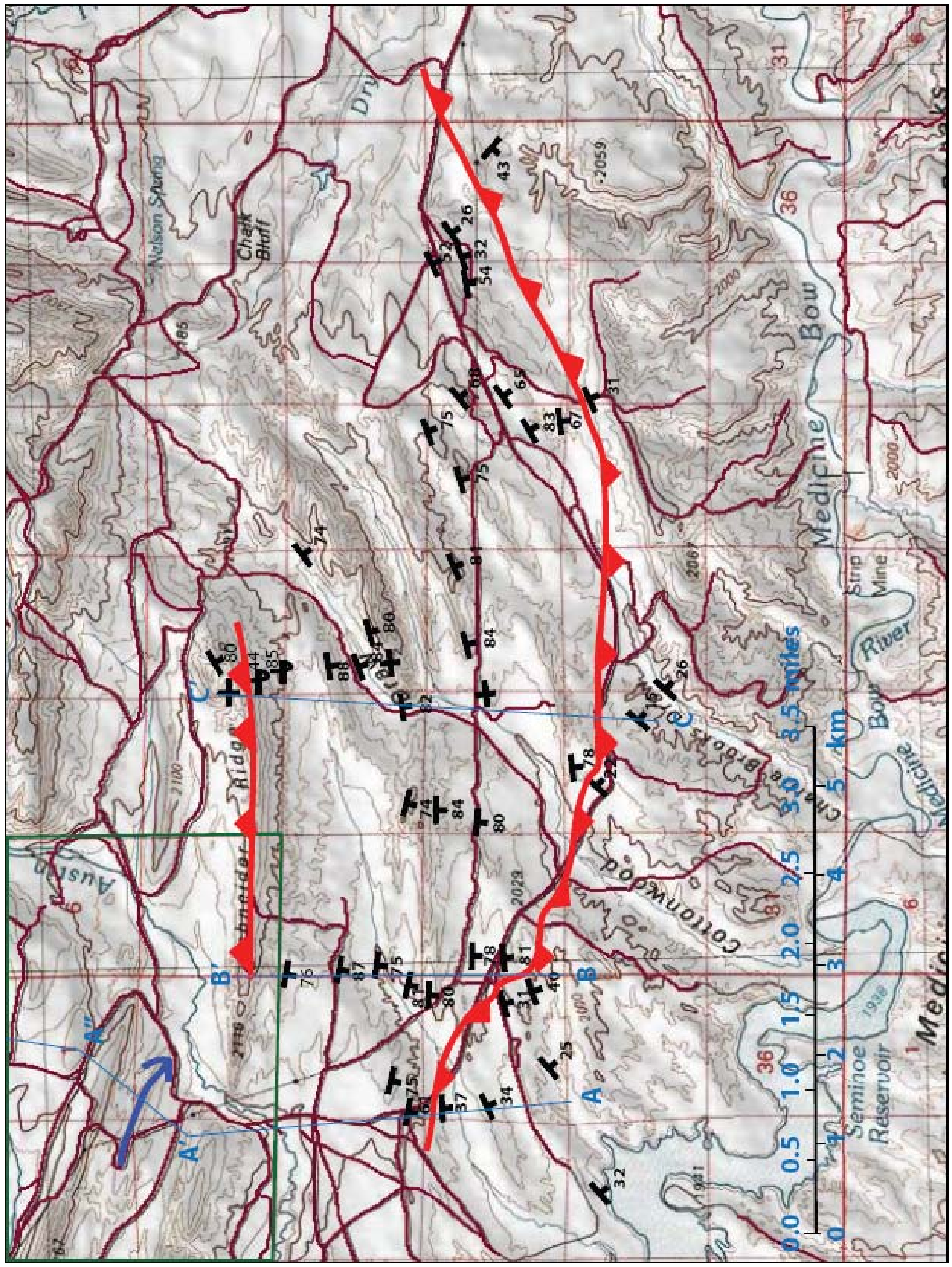
Nelson Spring
Chalk Bluff
Dry
Ridge
Cottonwood
Brooks
Medicine Bow
Bow
River
Strip Mine
Seminoe Reservoir
A
A'
A''
B
B'
C
C'
miles
km

Figure 6 A third representation of fault vergences in the study area. Both the Hanna-Leo Road fault in the south and the Schneider Ridge/Horseshoe Anticline fault in the north are south-verging splay thrusts. This structural map corresponds to the cross-section of Model 5 in Figure 21.

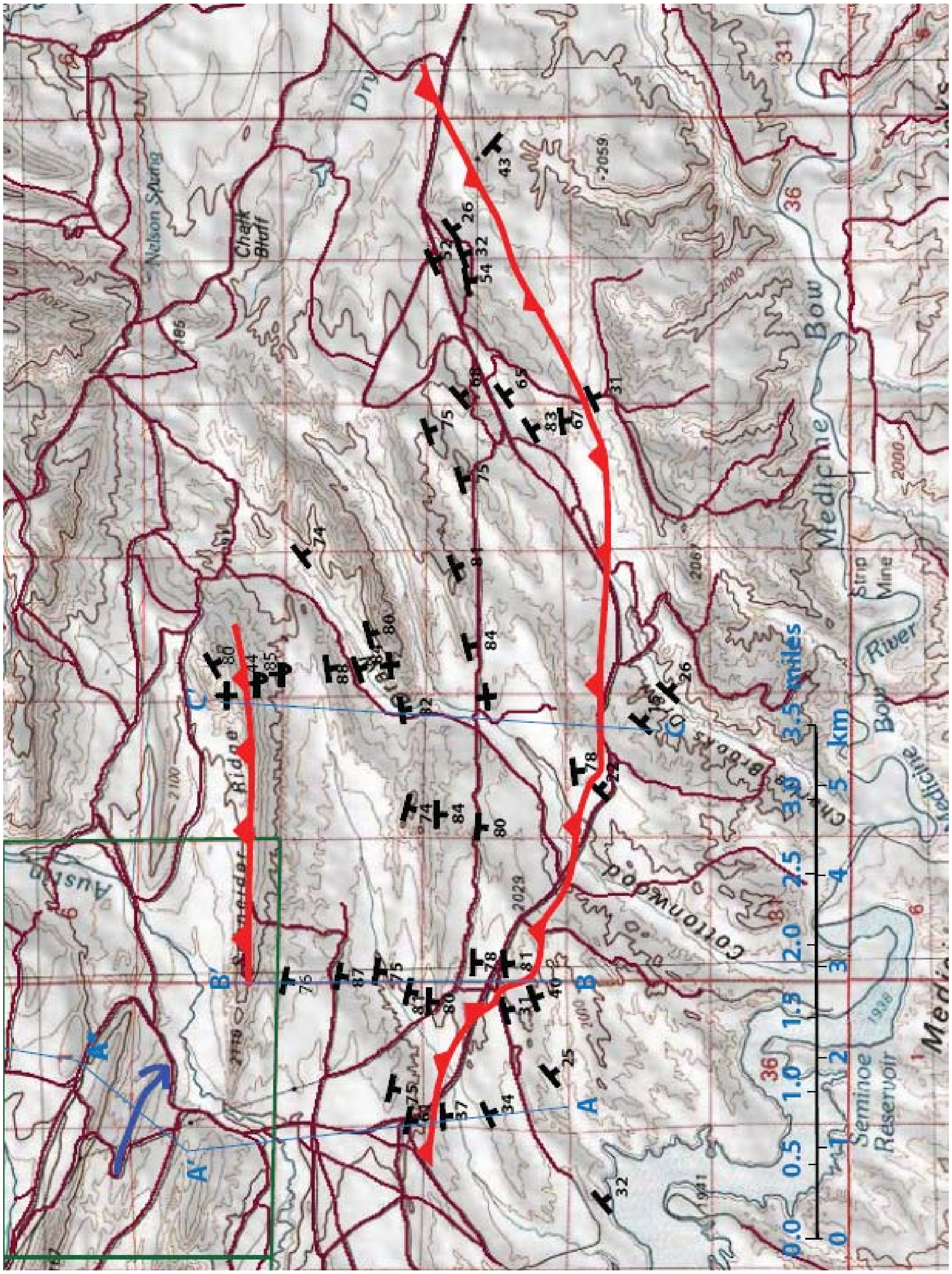

Nelson Spring
Chalk Bluff
Dry
Ridge
Austin
Cottonwood
Brooks
Medicine Bow
Bow River
Strip Mine
Seminoe Reservoir
A
A'
B
B'
C
C'
miles
km

Figure 7 From Erslev (1991). This diagram illustrates the trishear model of deformation. The layers closest to the fault elongate and shear, and the dips of these layers rotate to become closer to the dip of the fault plane. The trishear model allows for both heterogeneous and homogeneous deformation.

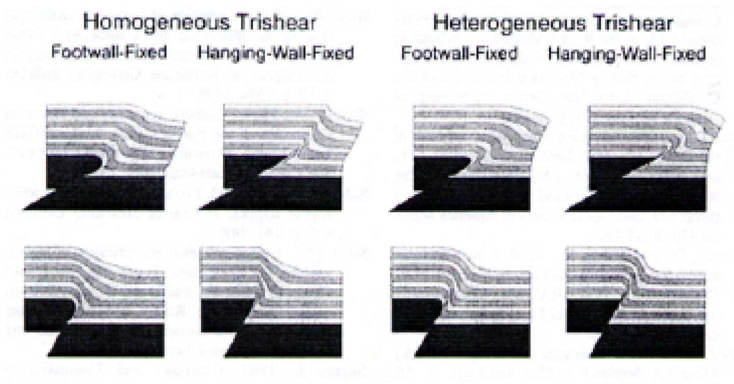
Homogeneous Trishear
Footwall-Fixed
Hanging-Wall-Fixed
Heterogeneous Trishear
Footwall-Fixed
Hanging-Wall-Fixed

Figure 8 From Sterne (2006). This figure illustrates the passive roof thrust model. A deep, blind master thrust and splay thrust system cause crowding in the foreland. To accommodate this, a number of oppositely-verging backthrusts develop. Over the top of these backthrusts, a passive roof thrust forms. Model 1 of this paper correlates best with this theory. The north-verging Schneider Ridge/Horseshoe Anticline fault (and related faults) are the faults contained within the triangle zone. The Hanna-Leo Road fault is the passive roof thrust, with a shallower dip than the north-verging faults in front of it.

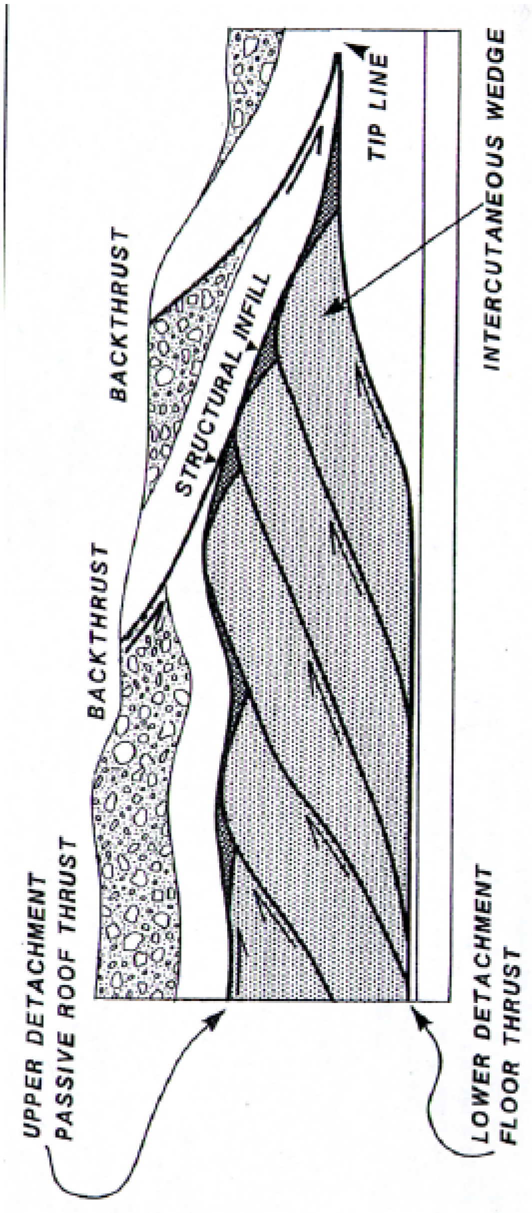
UPPER DETACHMENT
PASSIVE ROOF THRUST
BACKTHRUST
BACKTHRUST
STRUCTURAL INFILL
TIP LINE
INTERCUTANEOUS WEDGE
LOWER DETACHMENT
FLOOR THRUST

Figure 9 This series of cartoons illustrates, in a simplified manner, the hypothesis that the dips seen at the surface near the Hanna-Leo Road can be explained using an erosional unconformity rather than a fault. In Stage 1, the Shirley Thrust forms an anticline/syncline pair as it breaks toward the surface. As this structure is raised above sea level, it erodes, and the debris fills the syncline basin. Stage 2 shows how the syncline basin rotates as the Shirley Thrust continues to propagate. The debris deposited in the basin during this stage is deposited at an angle to the original debris. Stage 3 continues the rotation of the basin. The area in the bold circle is illustrated in Stage 4. The forelimb of the fault propagation fold is vertical to overturned at Schneider Ridge. The syntectonic basin fill from stages 2 and 3and forelimb have eroded away, but erosion continues in this stage and is deposited along the angular unconformity from Stage 2. This unconformity is what is now exposed along the Hanna-Leo Road. It follows the curve of the syncline basin margin.

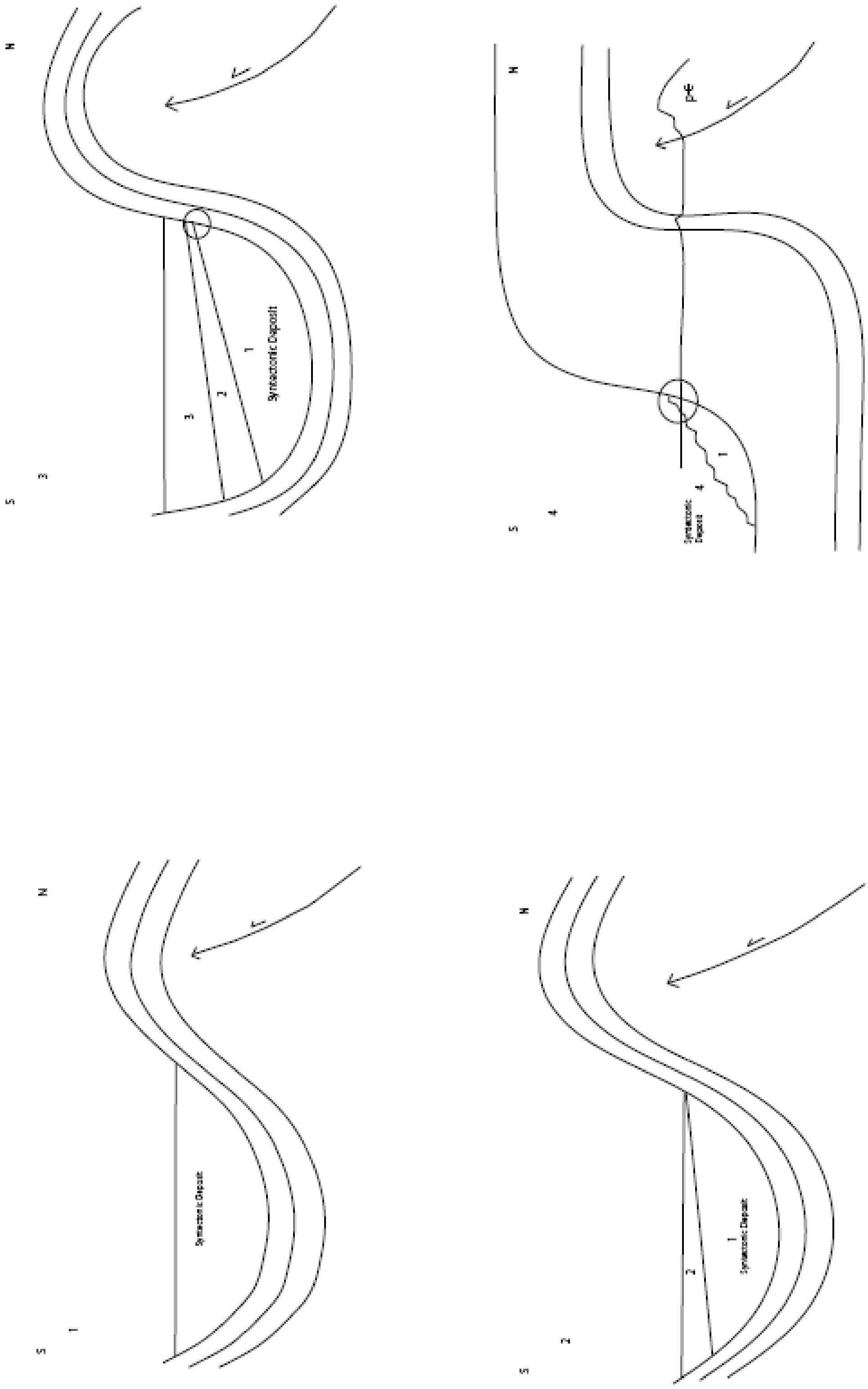
S
N
1
2
3
4
Syntectonic Deposit
P-Є

Figure 10 From Sterne (2006). This figure shows the evolution of the triangle zone, beginning with the undeformed state. Movement begins on the floor thrust, bringing older layers on top of younger layers. At the tip point, the backthrust begins to move in the original hanging wall, toward the hinterland, placing younger layers on older layers. Continued movement along the floor thrust causes crowding in the foreland, and a roof thrust develops over the backthrust wedge. This roof thrust can place both younger strata on older strata and older strata on younger strata.

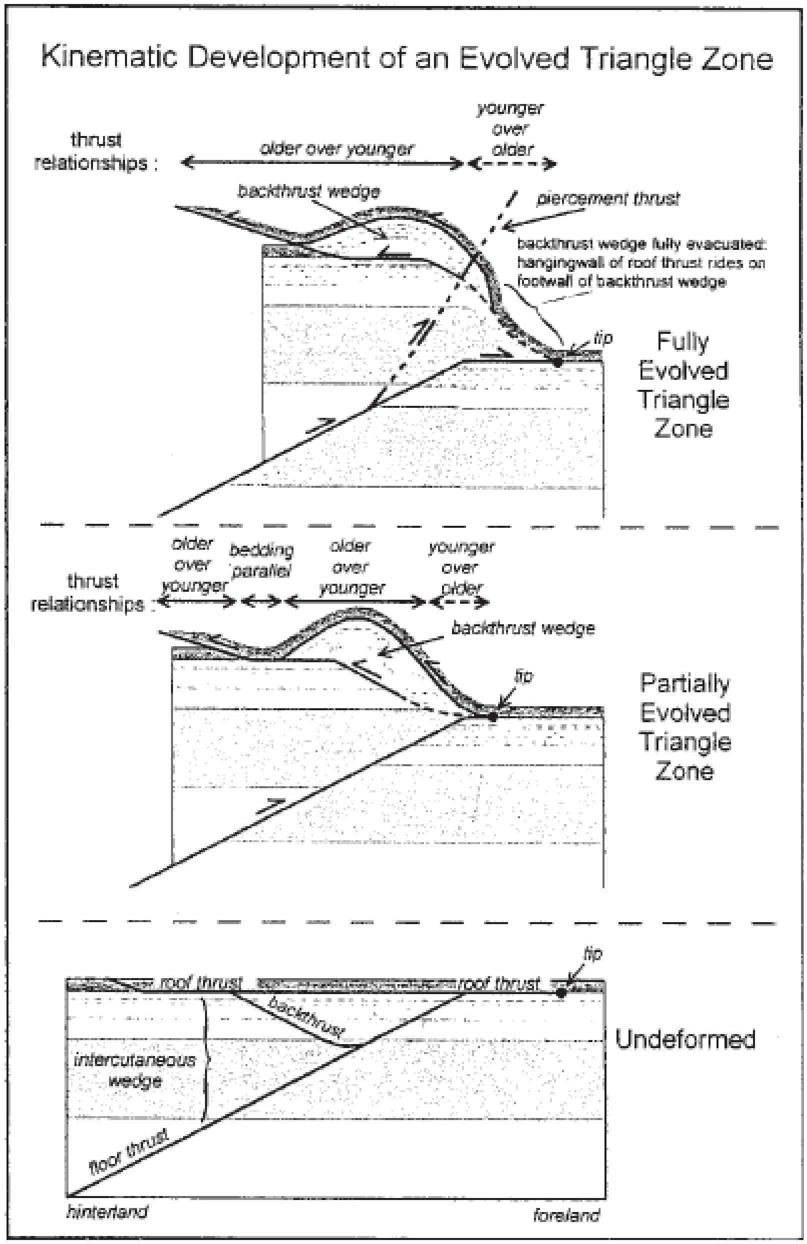
Kinematic Development of an Evolved Triangle Zone
younger over older
thrust relationships :
older over younger
backthrust wedge
piercement thrust
backthrust wedge fully evacuated: hangingwall of roof thrust rides on footwall of backthrust wedge
tip
Fully Evolved Triangle Zone
older over younger
bedding parallel
older over younger
younger over older
thrust relationships :
backthrust wedge
tip
Partially Evolved Triangle Zone
tip
roof thrust
roof thrust
backthrust
intercutaneous wedge
floor thrust
Undeformed
hinterland
foreland

Figure 11 From Taft (1997). This is the seismic data from Homan (Homan, 1988). The structural interpretations are Taft's hypothesis for the Horseshoe Ridge Anticline area. Taft's model was the basis for Model 1 of this paper.

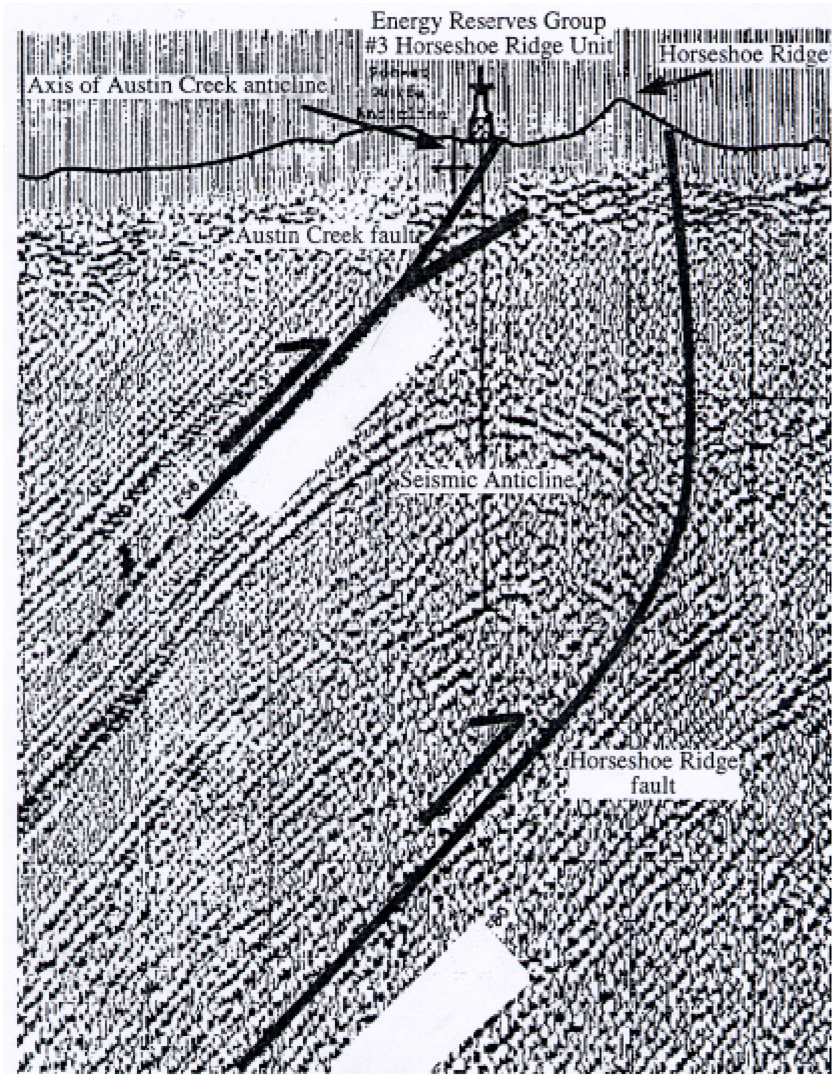
Energy Reserves Group
#3 Horseshoe Ridge Unit
Horseshoe Ridge
Axis of Austin Creek anticline
Austin Creek fault
Seismic Anticline
Horseshoe Ridge fault

Figure 12 Cartoon representation of the sequence of events that formed the Shirley Thrust. Movement began along a blind master thrust verging south. At some point a splay fault broke toward the surface, forming a fault propagation fold cored by the Precambrian metamorphics. The Shirley Fault broke to the surface, bringing the Precambrian up to its present height. The Paleozoic and Mesozoic sediments that had draped the Precambrian have eroded to expose the metamorphics as the Shirley Mountains.

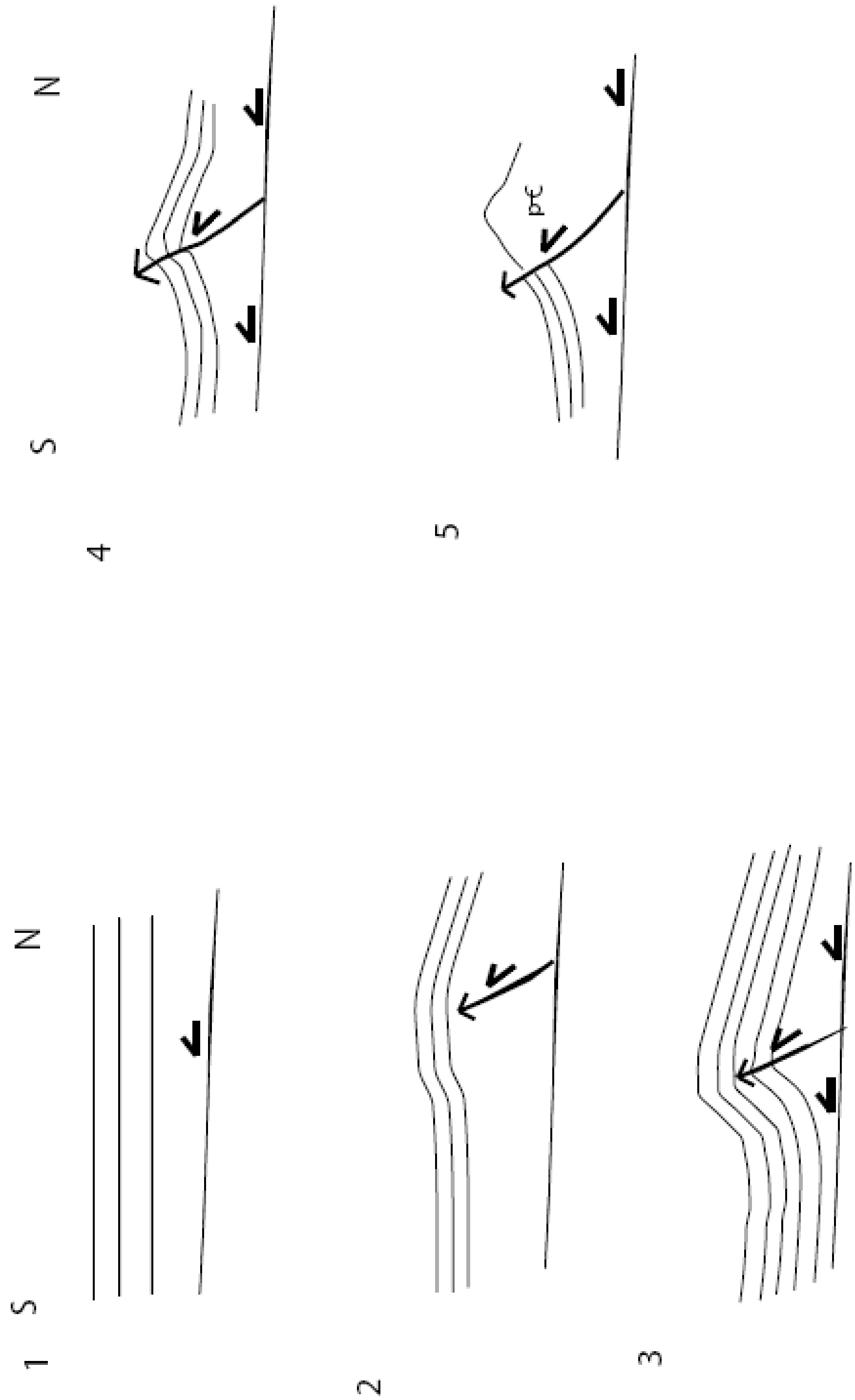

1
S
N
2
3
4
S
N
5

Figure 13 This figure continues from the sequence of events shown in Figure 12, and illustrates Model 1 in a simplified manner. After the Shirley Thrust reached the surface, movement continued along the blind master thrust, resulting in crowding in the foreland. The first north-verging out-of-the-basin fault forms at a shallow angle. Later, a second north-verging fault propagates through the first's footwall, tilting the first fault as it breaks to the surface. A third small splay fault develops on Schneider Ridge, resulting in the shifting of the layers on the south side of the ridge and causing some overturned bedding. This figure does not represent the Hanna-Leo Road fault as a shallower, passive roof thrust, as proposed by Sterne (Sterne, 2006).

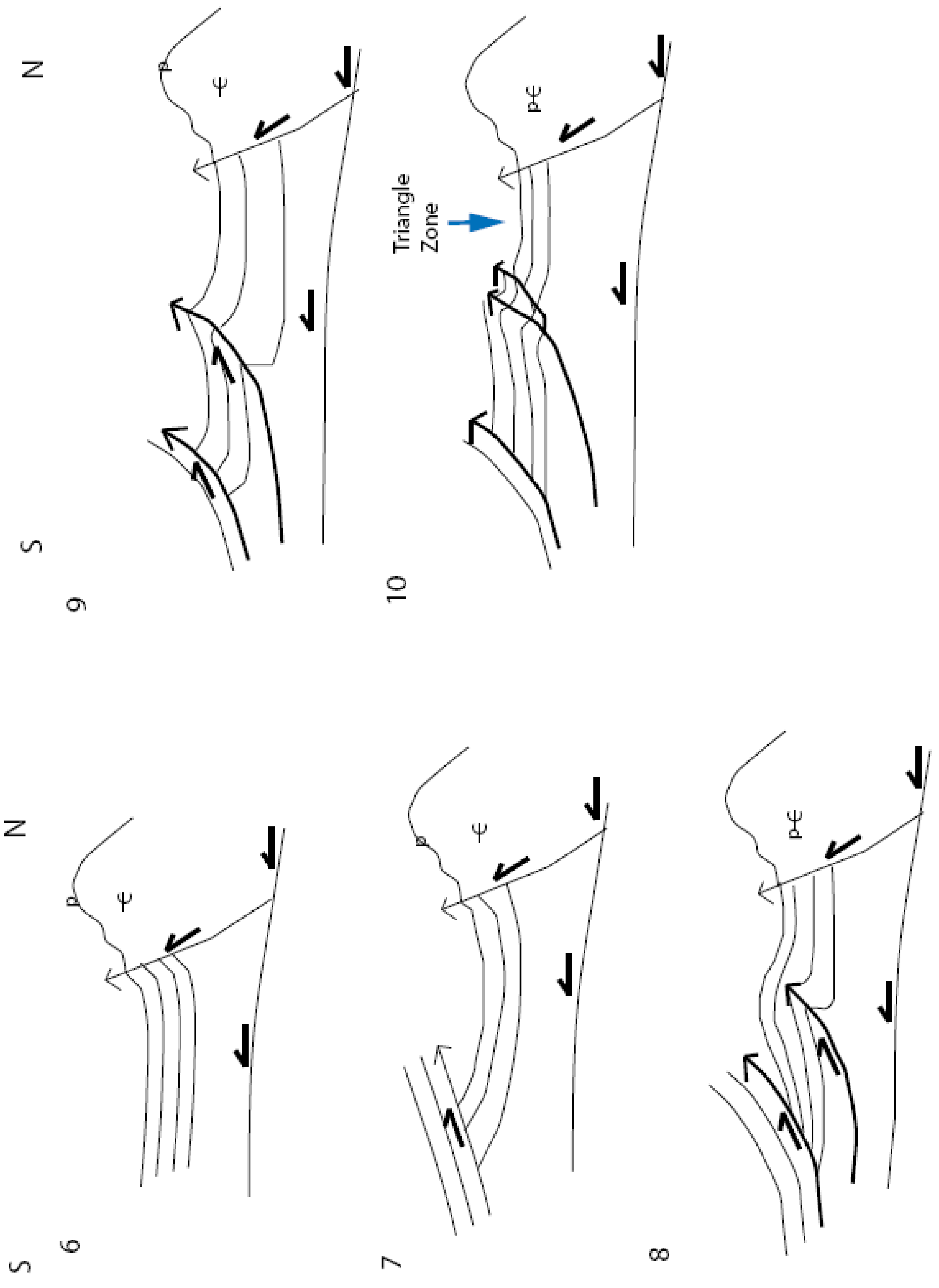

S
N
9
10
Triangle Zone
6
7
8

Figure 14 This is the cross-section for Model 1 along the transect A-A''', at scale 1:9600. This model shows the blind master thrust and Shirley Thrust as south-verging, and all other faults along the transect as north-verging, out-of-the-basin faults. The Hanna-Leo Road fault here is shown as a deep, steep fault similar to those that formed near the Horseshoe Anticline (between A'' and A'''). A better interpretation might follow Sterne's triangle zone model (**Figure 9**), and draw this fault as a shallow roof thrust that runs parallel to the bedding that dips about 30º in the south end of the transect, rather than running parallel to the bedding that dips about 75º.

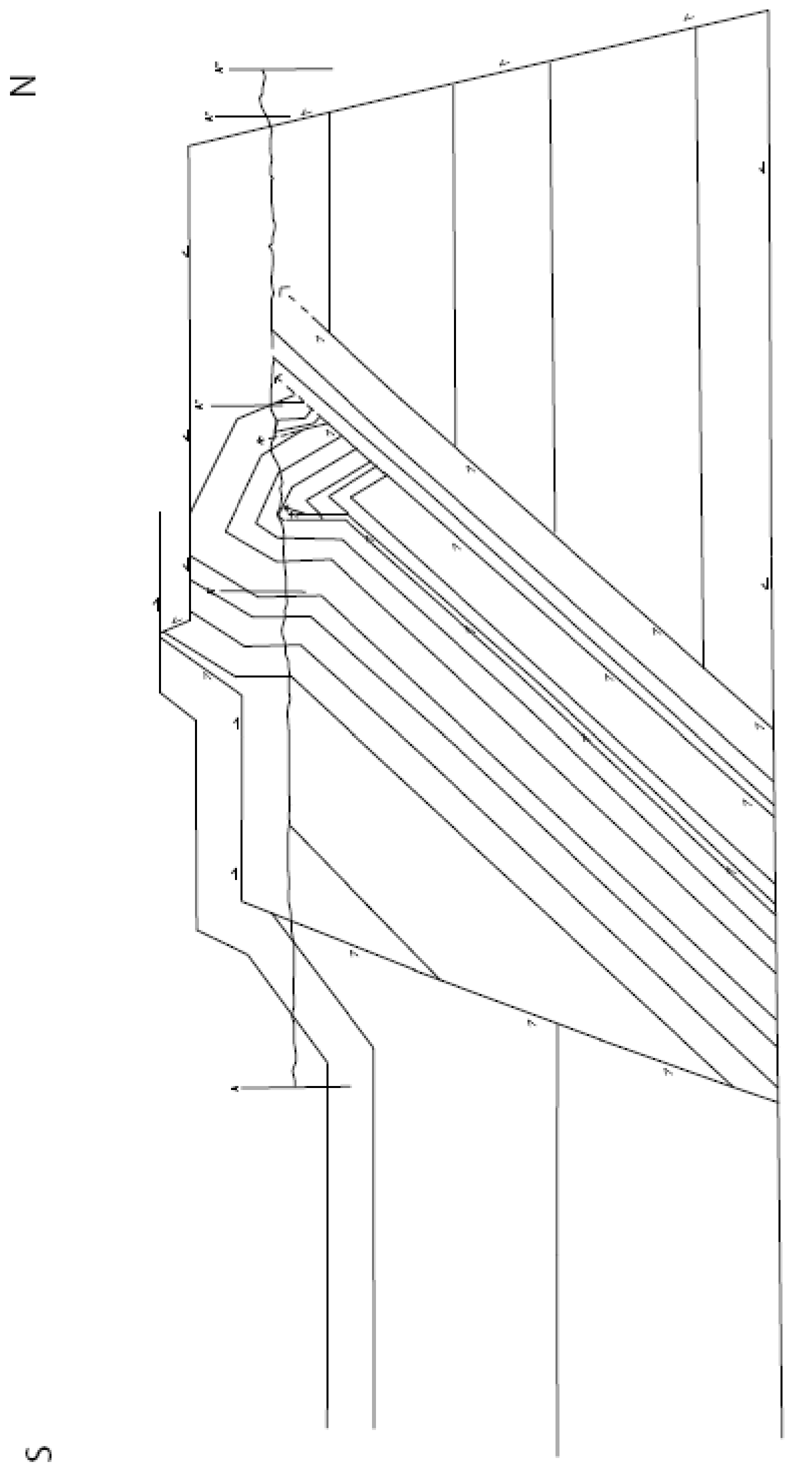
N
S

Figure 15 Model 1 illustrated along transect B-B', scale 1:9600. As in Figure 14, the out-of-the-basin faults are steep and north-verging. The complexity of Schneider Ridge (just south of B') is shown in a very simplified manner. The scale of this cross-section is not small enough to enable the geometries to be shown in a comprehensible manner.

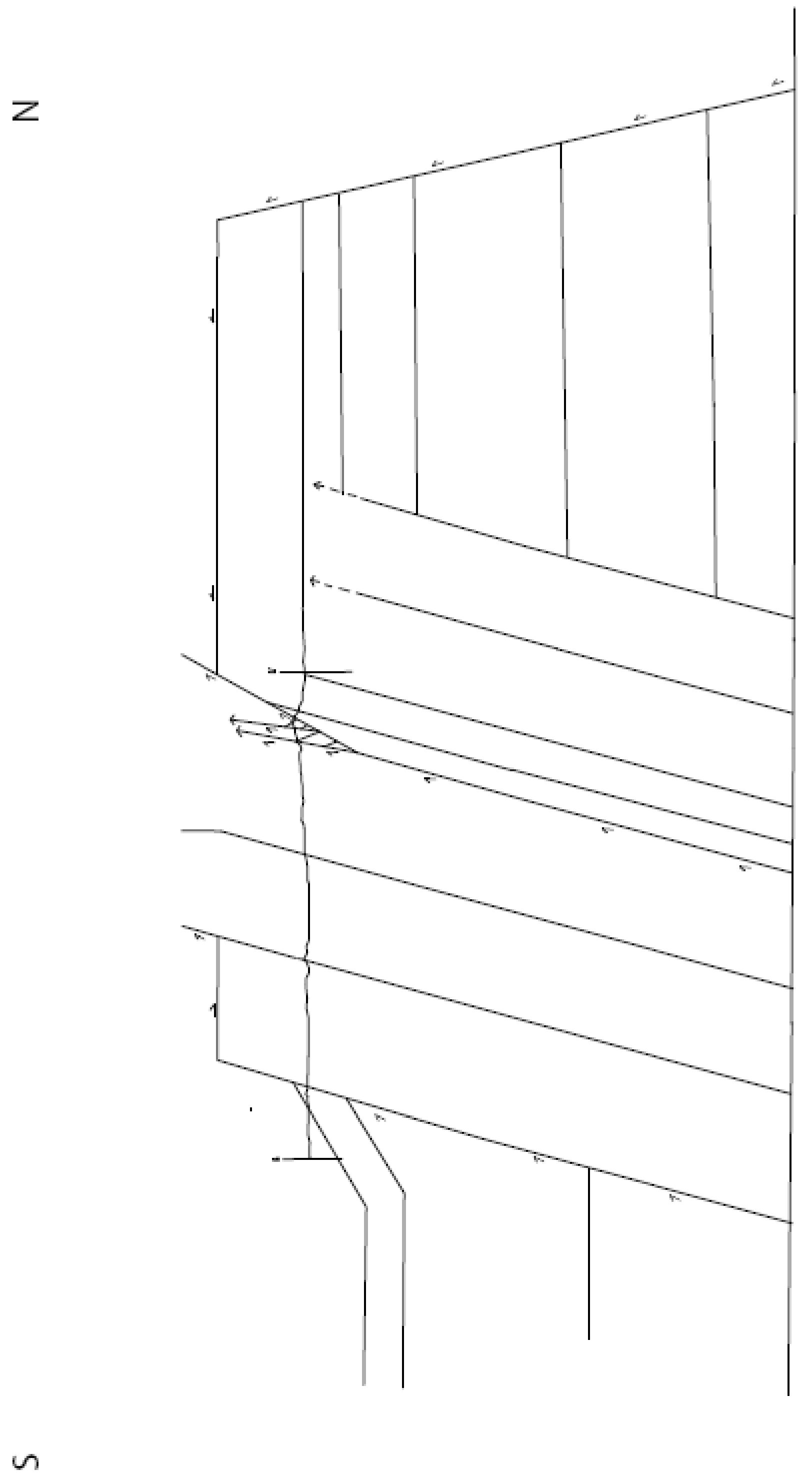
N
S

Figure 16 This figure is a continuation of the timeline from Figure 12. After the Shirley Thrust breaks to the surface, a smaller south-verging splay thrust breaks off the Shirley Thrust. This thrust forms a fault propagation fold (Horseshoe Ridge Anticline), and eventually breaks to the surface. Continued movement along the south-verging blind master thrust causes crowding in the basin, resulting the formation of a north-verging out-of-the-basin fault.

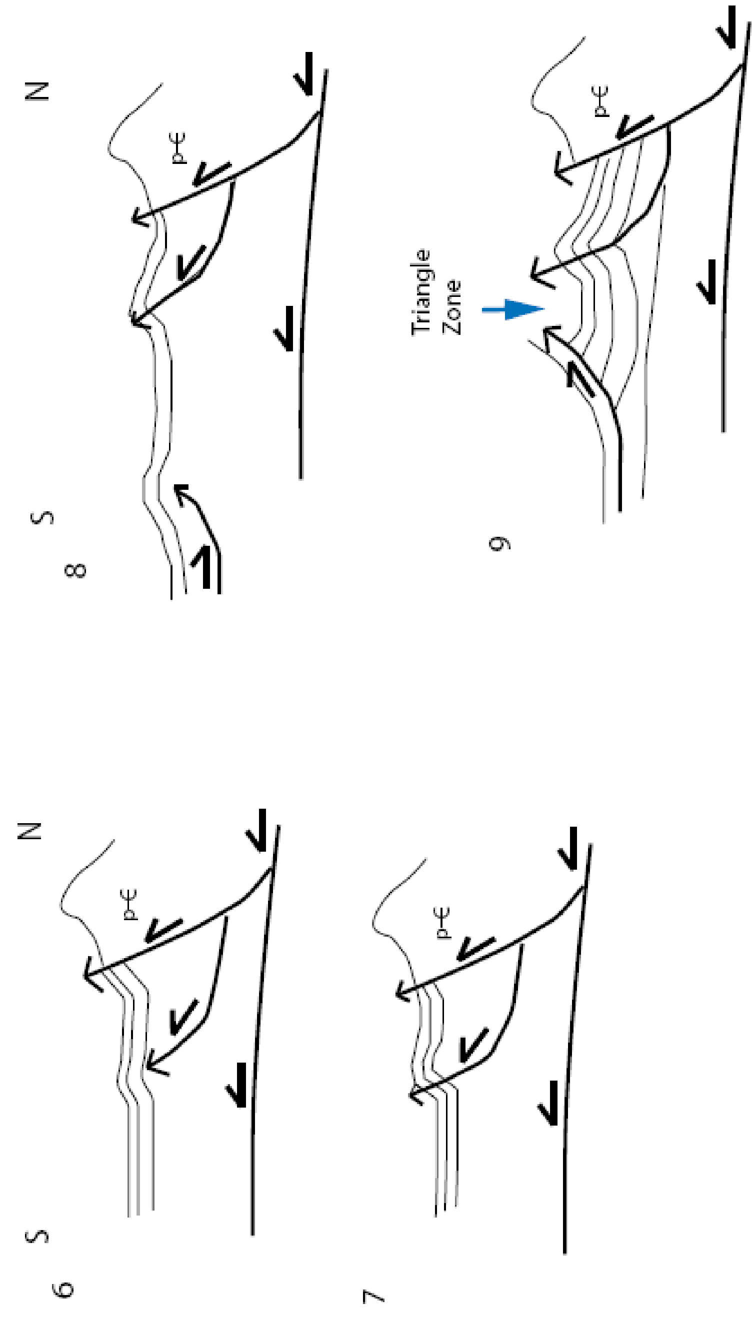

8
S
N
p-Є
9
Triangle Zone
6
S
N
p-Є
7
p-Є

Figure 17 This figure is the cross-section for Model 2 along transect A-A'''', scale 1:9600. Model 2 has the south-verging blind master fault and Shirley Thrust, The fault at the Horseshoe Anticline (between A' and A'') is drawn as a south-verging splay thrust off the Shirley Thrust in the north. This splay thrust created a fault propagation fold (the Horseshoe Ridge Anticline). The Hanna-Leo Road fault in the south is drawn as a north-verging out-of-the-basin fault. Unlike Figures 14 and 15, the fault in this figure follows the 30º dip of the bedding near the surface. The main problem in this cross-section is the northern tilt of the anticline in the footwall of the Shirley Thrust. This configuration seems incongruous with the movement of the south-verging master thrust beneath it. A more plausible model would have this anticline leaning south, as part of a anticline/syncline pair. The syncline would have been the footwall cutoff of the Shirley Thrust fault propagation fold.

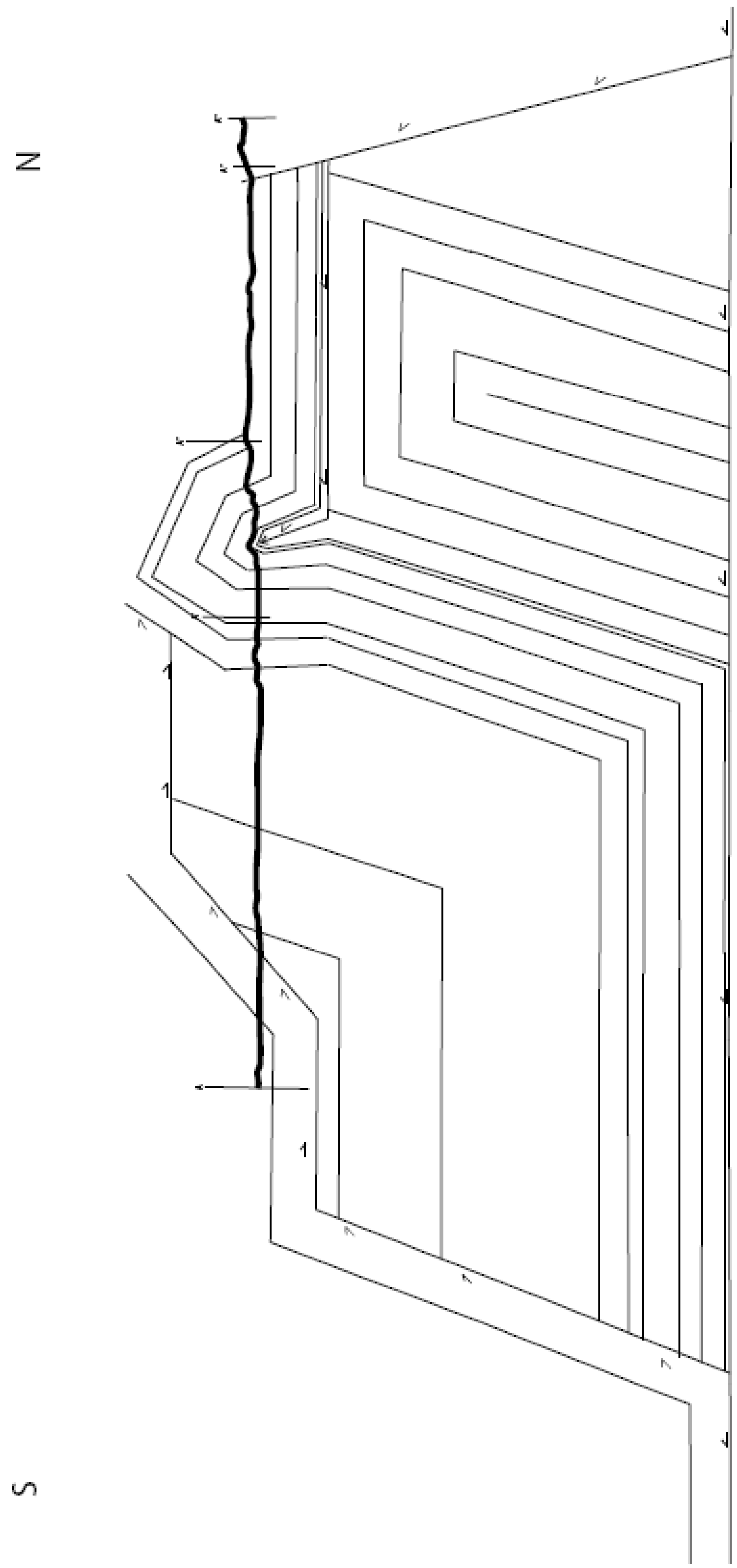
N
S
1
1
1

Figure 18 Model 2 illustrated along transect B-B', scale 1:9600. As in Figure 16, the fault that forms Schneider Ridge (just south of B') is a south-verging splay off the Shirley Thrust. Again, the complex geometries of Schneider Ridge are not illustrated here. The Hanna-Leo Road in the south is a north-verging out-of-the-basin fault that runs parallel to the 30º bedding at the surface.

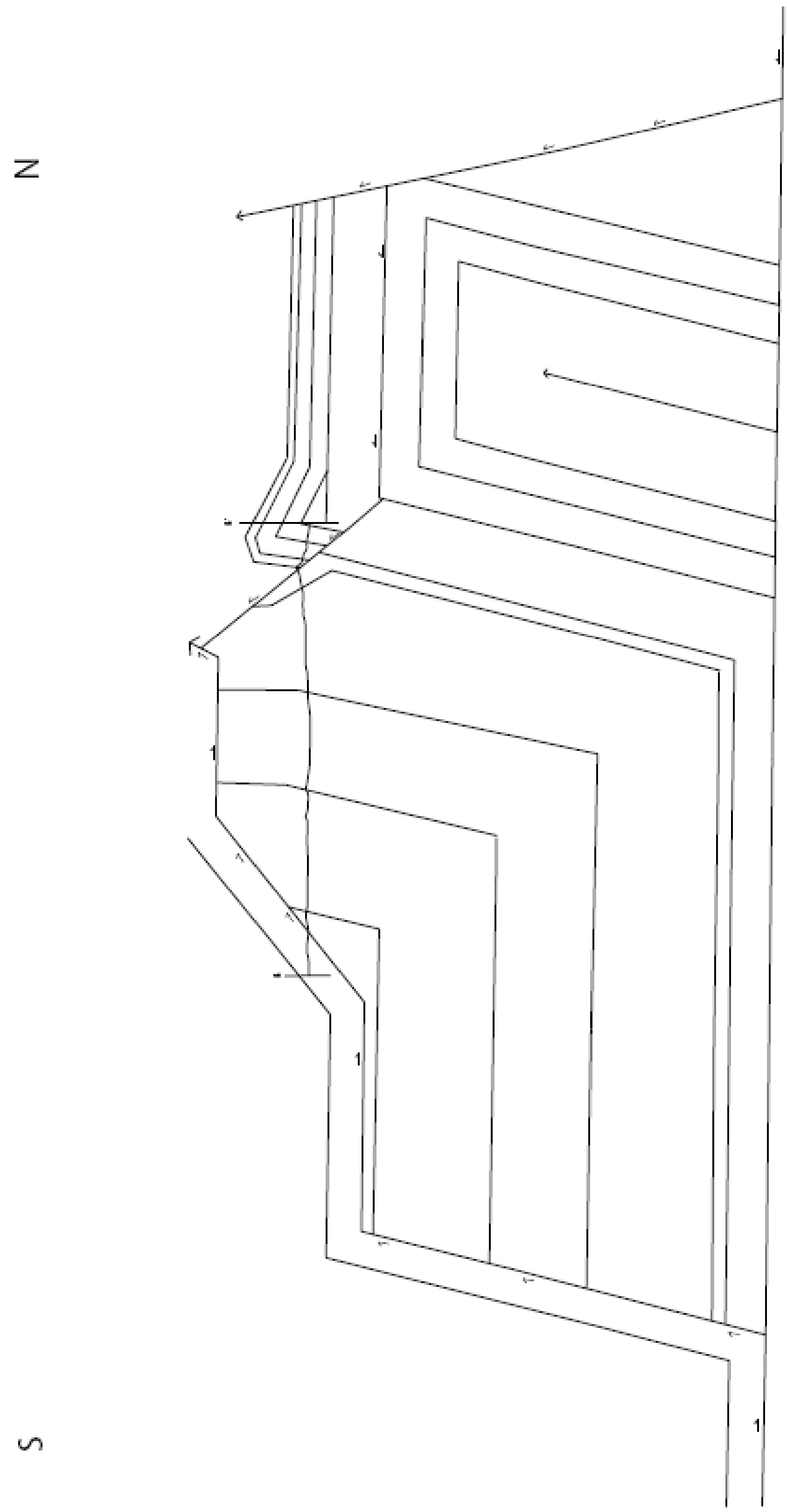
N
S

Figure 19 Model 2 illustrated along transect C-C', scale 1:9600. This figure is very similar to Figure 17, as the two transects are relatively close. It features a south-verging blind thrust and Shirley Thrust, and a south-verging splay fault forming Schneider Ridge (at C'). The Hanna-Leo Road fault is a north-verging out-of-the-basin fault that runs parallel to the 30º bedding at the surface.

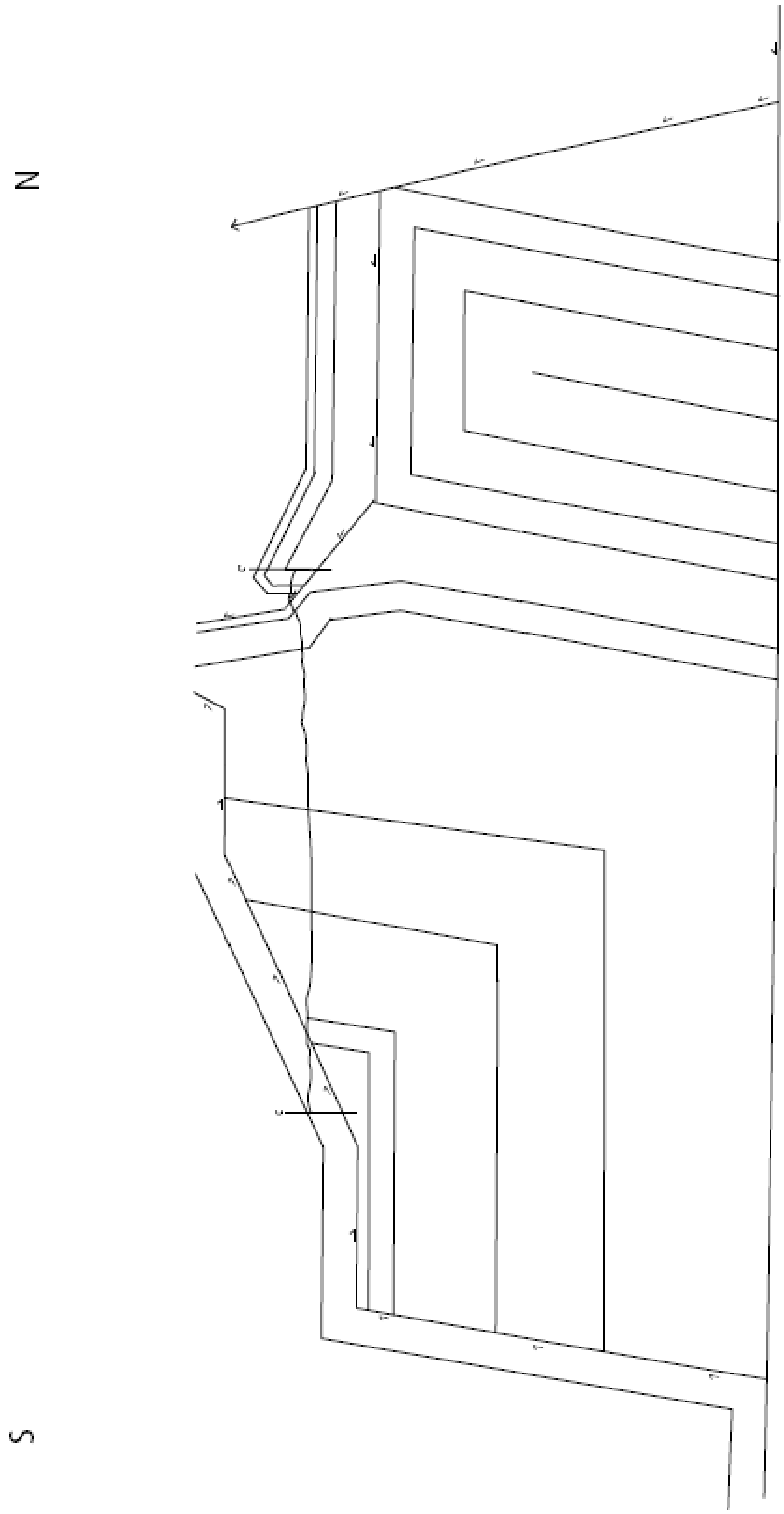
N
S
1
1

Figure 20 This is the cross-section for Model 3 along transect A-A'''', scale 1:9600. Model 3 features the same fault vergences as Model 2. Unlike Figure 16, the anticline in the footwall of the Shirley Thrust (below A''') is south-leaning, which corresponds with the movement along the master fault beneath it. Rather than breaking off the Shirley Thrust near the surface, the fault that forms the Horseshoe Anticline breaks off near the master fault and comes up to the surface steeply. According to this model, the fault truncates the anticline below it, which is unlikely in reality. The Hanna-Leo Road fault is a north-verging, out-of-the-basin fault that runs parallel to the 30º bedding at the surface.

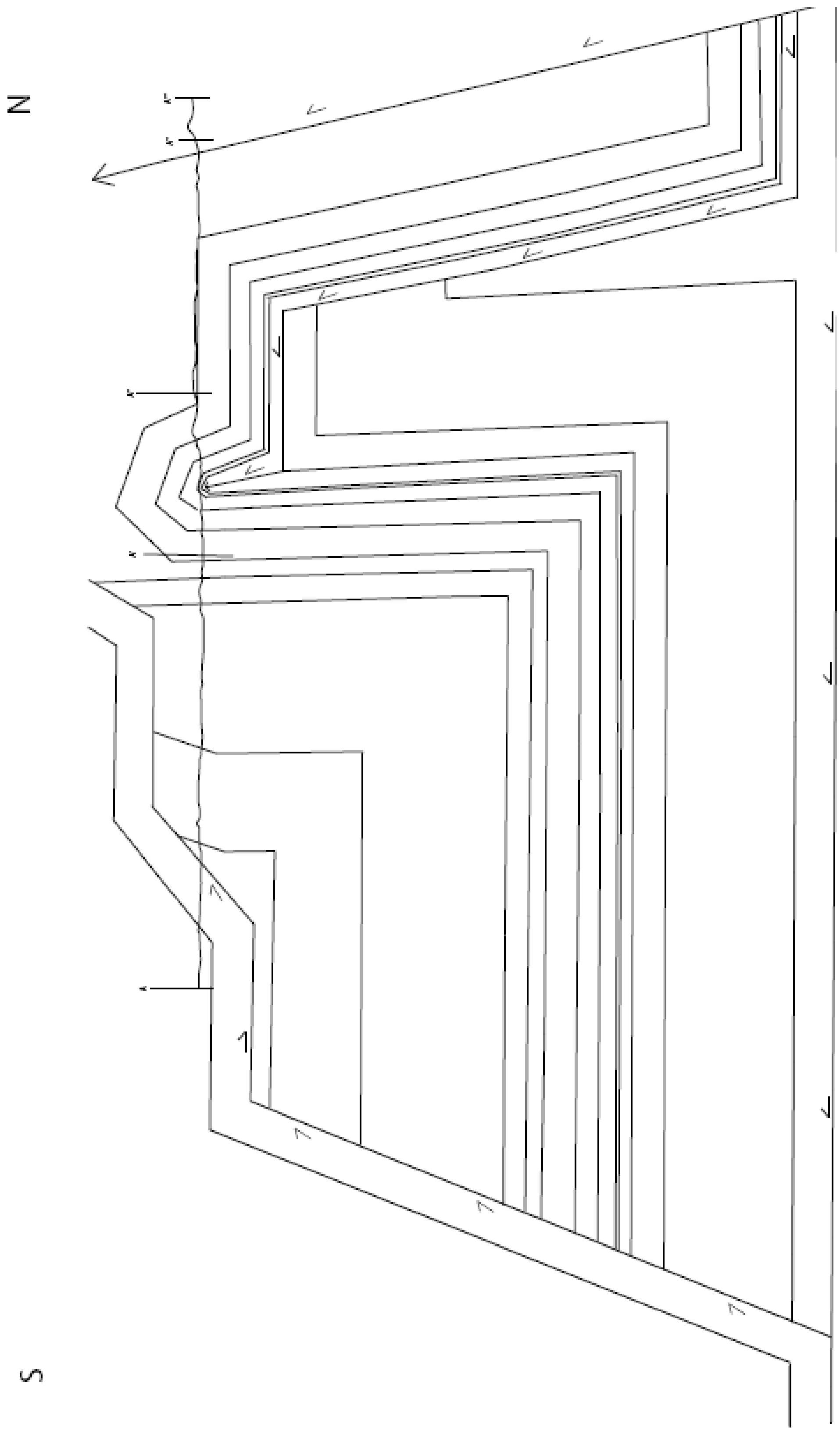
N
S

Figure 21 This is the cross-section for Model 4 along transect A-A''', scale 1:9600. This model has the south-verging blind master fault and Shirley Thrust, and illustrates the fault creating the Horseshoe Ridge Anticline as a shallow splay off the Shirley Thrust. This model corrects the truncation of the footwall anticline seen in Model 3 (**Figure 19**). The Hanna-Leo Road fault is a north-verging, out-of-the-basin fault that runs parallel to the 30º bedding at the surface.

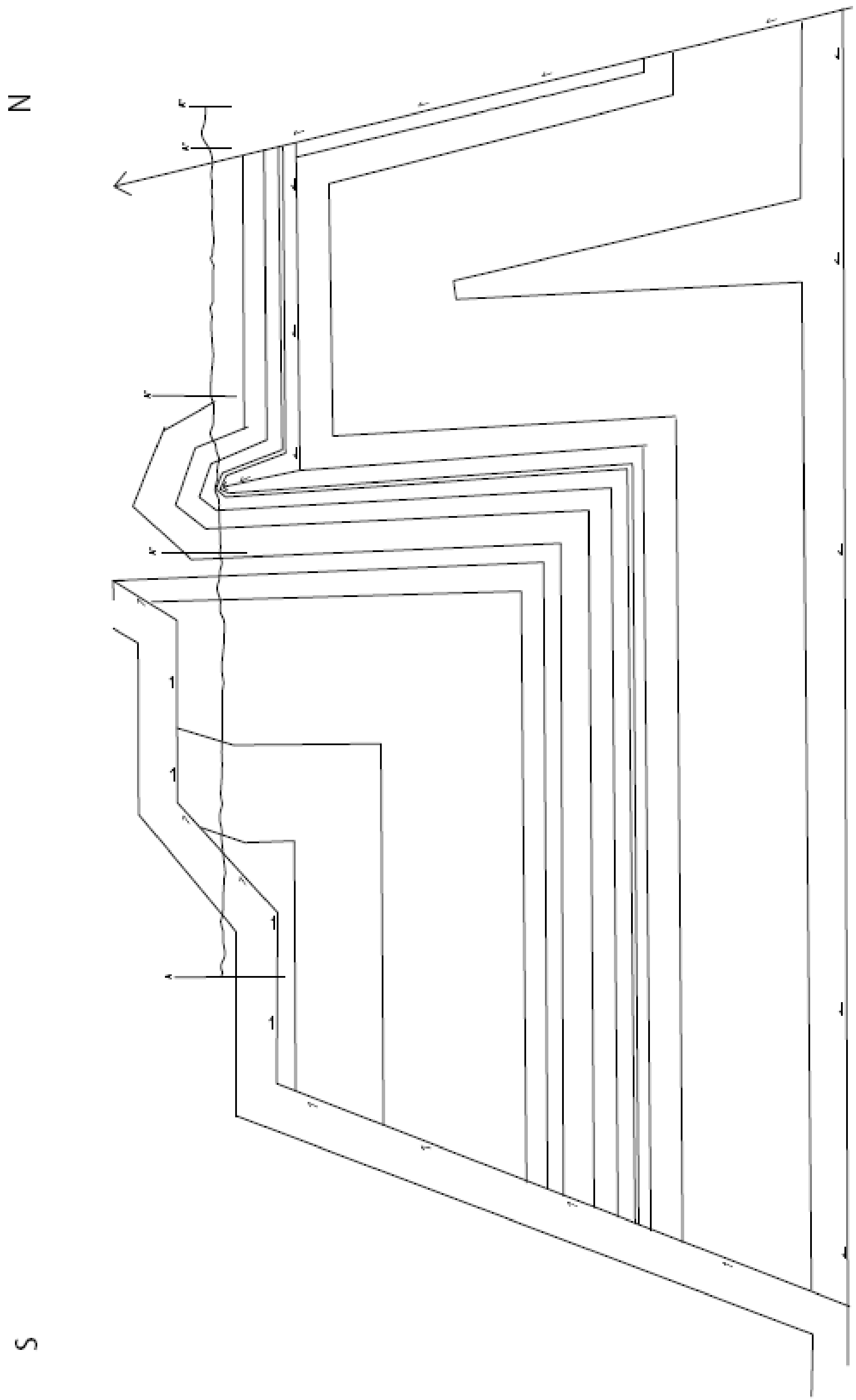
N
S

Figure 22 This is the cross-section for Model 5 along transect B-B', scale 1:9600. This model has a south-verging thrust fault forming a fault propagation fold at Schneider Ridge (at B'). A second fault propagates through the footwall and breaks to the surface at the Hanna-Leo Road. There are significant problems with this model. The block between the two faults is truncated by the second fault. It seems unlikely that a fault would run nearly parallel to bedding. A better model may have this block rotated rather than truncated. However, since the beds are not overturned and dipping to the south, they would have needed a north-verging master fault to rotate them to their current position. The overturned beds on Schneider Ridge are depicted as footwall drag from the south-verging fault that runs over them. The area beneath the faults poses a challenging geometry that was not balanced successfully. Because of the problems with this particular cross-section, this model was not attempted on the other two transects.

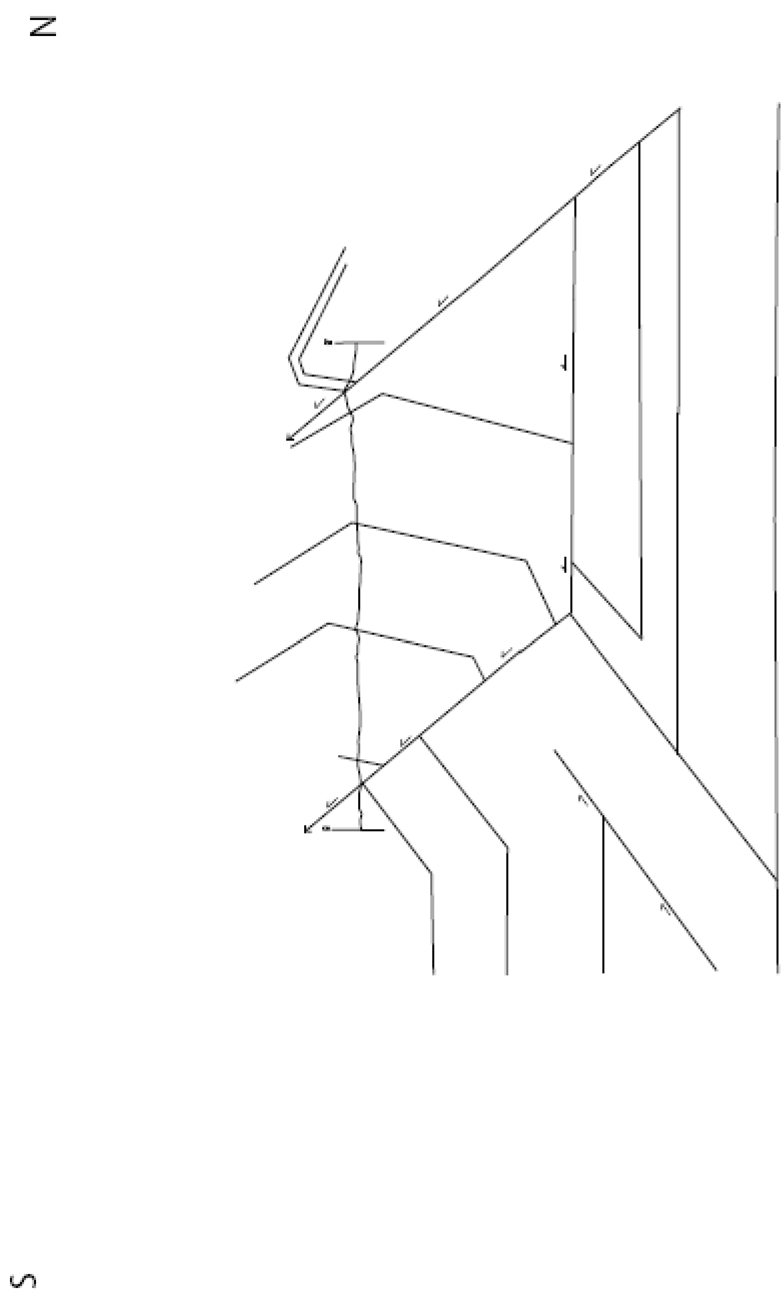
N
S